Effect of Nitrogen on the Structure and Composition of Primordial Organic Matter Analogs

Pauline Lévêque, Clémence Queffelec, Christophe Sotin, Carlos Afonso, Olivier Bollengier, Adriana Clouet, Erwan Le Menn, Yves Marrocchi, Isabelle Schmitz, Bruno Bujoli

ACS EARTH AND SPACE CHEMISTRY

http://pubs.acs.org/journal/aesccq
Article

Effect of Nitrogen on the Structure and Composition of Primordial Organic Matter Analogs

Pauline Lévêque,* Clémence Queffelec, Christophe Sotin,* Carlos Afonso, Olivier Bollengier, Adriana Clouet, Erwan Le Menn, Yves Marrocchi, Isabelle Schmitz, and Bruno Bujoli

Cite This: https://doi.org/10.1021/acsearthspacechem.3c00311

ABSTRACT: Organic molecules are ubiquitous in primitive solar system bodies such as comets and asteroids. These primordial organic compounds may have formed in the interstellar medium and in protoplanetary disks (PPDs) before being accreted and further transformed in the parent bodies of meteorites, icy moons, and dwarf planets. The present study describes the composition of primordial organics analogs produced in a laboratory simulator of the PPD (the Nebulotron experiment at the CRPG laboratory) with nitrogen contents varying from N/C < 0.01 to N/C = 0.63. We present the first Fourier transform ion cyclotron resonance mass spectrometry analysis of these analogs. Several thousands of molecules with masses between m/z 100 and 500 are characterized. The mass spectra show a Gaussian shape with maxima around m/z 250. Highly condensed polyaromatic hydrocarbons (PAH) are the most common compounds identified in the samples with lower nitrogen contents. As the amount of nitrogen increases, a dramatic increase of the chemical diversity is observed. Nitrogen-bearing compounds are also dominated by polyaromatic hydrocarbons (PANH) made of 5- and 6-membered rings containing up to four nitrogen atoms, including triazine and pyrazole rings. Such N-rich aromatic species are expected to decompose easily in the presence of water at higher temperatures. Pure carbon molecules are also observed for samples with relatively small fractions of nitrogen. MS peaks compatible with the presence of amino acids and nucleobases, or their isomers, are detected. When comparing these Nebulotron samples with the insoluble fraction of the Paris meteorite organic matter, we observe that the samples with intermediate N/C ratios bracketing that of the Paris insoluble organic matter (IOM) display relative proportions of the CH, CHO, CHN, and CHNO chemical families also bracketing those of the Paris IOM. Our results support that Nebulotron samples are relevant laboratory analogs of primitive chondritic organic matter.

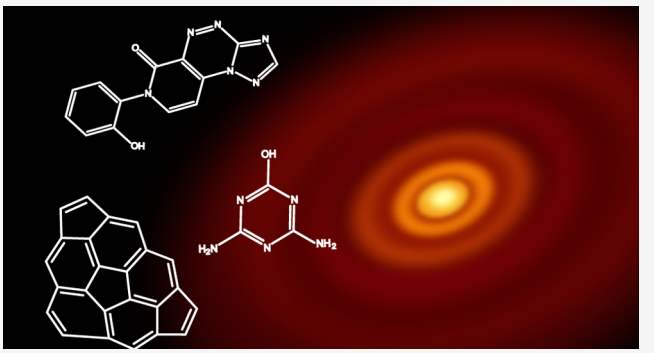

KEYWORDS: *primordial organic molecules, FT-ICR MS, structural analysis, Nebulotron, protoplanetary disk chemistry*

1. INTRODUCTION

Complex organic molecules abound in primitive objects of the solar system. Analysis of meteorites has long revealed the abundance of organics (up to 6 wt %) in carbonaceous chondrites,[1−7] with an insoluble fraction rich in the O−N−S heteroatoms.[3,8,9] Ultracarbonaceous Antarctic micrometeorites (UCAMMs), which are thought to be the remnants of the outer reaches of the solar protoplanetary disk (PPD), are very rich in organics: sliced samples show area ratios of silicium (the rocky matrix) to C═C aromatic bonds (the organic matter) of about 1/2 on average, with a large variability from 0 (pure aromatics) to 3.[10−12] In the past decades, in addition to telescope observations, the *in situ* examination of comets and asteroids and the analysis of their returned samples have also been made possible by dedicated space missions. The Rosetta mission revealed that dust particles from comet 67P/Churyumov-Gerasimenko were composed of up to 45 wt % of organic materials,[13] likely as complex molecular compounds similar to those found in carbonaceous chondrites.[14] Thermal dust models of 33 comets based on data by the Spitzer Space Telescope suggest a comparable abundance of carbon in many comets.[15] Part of the interest for the organic molecules found in primitive bodies stems from astrobiology, as meteorites have long been known to contain many molecules of astrobiological interest, such as nucleobases[16] and amino acids[17] (the so-called "building blocks of known life"). These molecules are also found in comets. Notably, isotopic analyses have confirmed the presence of glycine in the particles collected from the coma of 81/Wild2 by the Stardust spacecraft.[18] Most recently, several

Received: November 5, 2023
Revised: April 12, 2024
Accepted: April 12, 2024

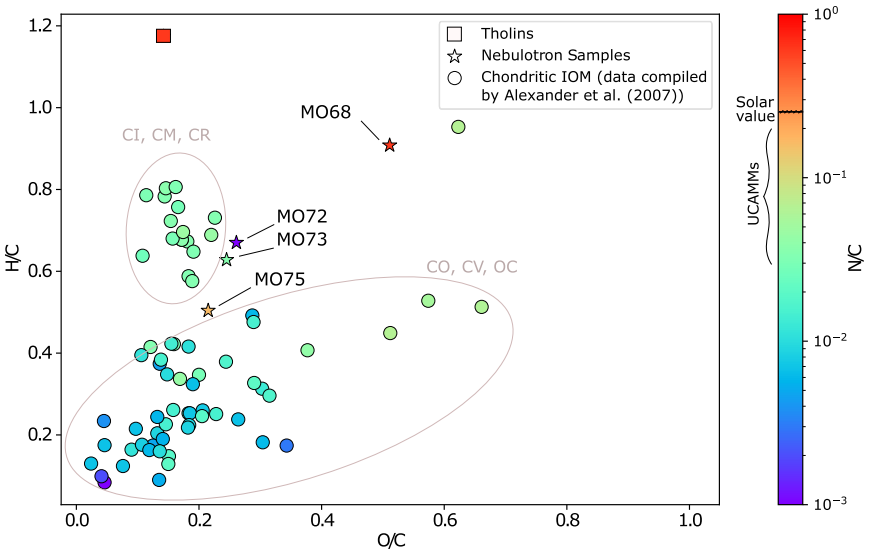

Figure 1. Comparison of the CHNO composition of the Nebulotron samples (our data) with carbonaceous chondrites IOM (data compiled by Alexander *et al.*[3]) in an H/C, O/C, and N/C elemental ratio plot. The N/C color scale displays the solar N/C value of 0.24[51] and the N/C range for UCAMMs.[12]

nucleobases and amino acids were also identified in the samples returned from the Ryugu asteroid (a body similar in composition and mineralogy to CI chondrites) by the Hayabusa2 mission.[19−22]

At least four processes have been proposed for the formation of primordial organic matter in PPDs, in particular in the solar system. These processes should likely be seen as complementary, as they may operate in different regions of PPDs and at different stages of their evolution.[23] A first mechanism to produce early organic molecules could be the electron, proton, or ion irradiation of mixtures of H−C−N−O-bearing ices (*e.g.*, H_2O, CO, and CH_4) with or without silicates.[24−27] This mechanism could only take place at the lower temperatures at which ices are stable (*e.g.*, the saturation vapor pressure of H_2O nears 200 K at 1 Pa and decreases significantly at lower pressures).[28] However, this process would not be limited to the colder regions of PPDs; ices could also form and be irradiated in molecular clouds in the interstellar medium (ISM) before being incorporated into the PPDs where they would experience variable sublimation and isotopic exchanges with the gases of the disk due to their different sublimation temperatures.[29] This pathway is supported by mid-infrared observations of volatile precursors of organics in the ISM and in protostellar nebulae[30,31] and by the values for the D/H ratio and $^{15}N/^{14}N$ isotopic fractionation ratio that appear similar in the organic matter from (presolar) interplanetary dust particles and in the organic fraction of meteorites and comets.[32,33] As a second mechanism, organic molecules might be produced through the ionization of volatile species such as CO, N_2, and H_2 (and the reaction of their byproducts) directly in the gas phase, with N_2 being the main expected N carrier in all PPDs scenarios.[34−36] This process requires hotter environments such as the outer layers of PPDs, where temperatures are expected to reach 1000 K.[37] A third mechanism may be available at more moderate temperatures through Fischer−Tropsch-like reactions: in the presence of metal catalysts, and possibly in the presence of ammonia, CO and H_2 readily combine to produce hydrocarbons.[38−40] Finally, complex organics may also result from aqueous alteration of precursor materials, likely within asteroid parent bodies.[13,35,36] Proposed pathways include the polymerization of formaldehyde[41−43] or the alteration of HMT (hexamethylenetetramine—$C_6H_{12}N_4$).[44−46] However, a recent comprehensive characterization of the hydrogen isotopic composition of water-rich chondrites suggests that their IOM experienced minimal modification during fluid circulation.[47]

All four processes described above have been successfully implemented in laboratory experiments to produce synthetic samples mimicking part of the compositional and structural properties of chondritic organics. These analog samples thus offer a unique opportunity to explore how the range of chemo-physical conditions (temperature, molecular abundances, and irradiation regime) found in PPDs may influence the properties of the resulting primordial organic matter. To explore this causation, we study the organic samples produced by the Nebulotron experiment at the CRPG laboratory. This experiment produces synthetic analogs of primordial organics by means of a plasma reaction chamber, wherein a gas mixture is ionized at elevated temperatures (following a process akin to the second pathway described above).[48−50] Though this experiment relies on the ionization of gas mixtures through a microwave discharge plasma rather than through UV photo-dissociation, Nebulotron samples have nonetheless reproduced key properties of chondritic organics. First, by working with various gas mixtures of H_2, CO, and N_2, a variety of organic compositions have been generated that have reproduced part of the range of the H−C−N−O-dominated elemental abundances of solar PPD organics. As will be detailed and discussed throughout this article, this is especially true regarding nitrogen, as the Nebulotron samples used in this study present a range of N/C ratios from below 0.01 to 0.63. This range covers the lower N/C ratio of the IOM contained in CI chondrites (up to 0.06),[3,51] the higher N/C ratio of ultracarbonaceous Antarctica micro meteorites (up to 0.20),[12] the recommended N/C ratio for the solar system (0.24),[51] but also even higher values pertaining to contemporary organics produced in nitrogen-rich planetary atmospheres, such as Titan's organic haze produced by photochemistry in its upper atmosphere with N/C ratios between 0.06 and 0.8 depending on the formation process.[52] Tholins are laboratory analogs of Titan's haze; those referenced later in this study have a N/C

https://doi.org/10.1021/acsearthspacechem.3c00311
ACS Earth Space Chem. XXXX, XXX, XXX−XXX

ratio of 0.62 (Figure 1). Second, addition of noble gases in the gas mixtures led to the synthesis of organics showing Kr and Xe elemental and isotopic fractionation ratios similar to that of the organics-related Q phase found in chondrites.[34] Finally, gas chromatography-mass spectrometry (GC-MS) and Curie Point Pyrolysis GC-MS have shown that Nebulotron organics include many astrobiologically relevant molecules (such as amino acids and nucleobases) detected in meteorites and comets.[19] While these results illustrate the relevance of the Nebulotron samples in exploring the synthesis of primordial organics forming in PPDs, the detailed molecular composition of these samples, however, remains largely unknown. Combined with elemental analyses, such information would provide a better understanding of the relationship between the composition of PPDs and the nature of the resulting organics and some better insight into the chemo-physical properties of the early solar organic matter: notably, the reactivity of early organic matter to temperature and water will control its fate during the formation of primitive small bodies and, later, of planets and moons.

To fill that gap, the present study provides the first ultrahigh-resolution mass spectrometry investigation of Nebulotron organic samples, with a description of the organic molecules produced in an environment that simulates the conditions of the most intensely irradiated, outer layers of PPDs. A particular focus of the present work is to explore the relationship between the N content of the organic matter and its resulting structural features, in particular regarding the formation of PANHs[53] and of potential precursors of building blocks of life. To that end, the four Nebulotron samples selected for this study present a large range of nitrogen abundances (N/C from below 0.01 to 0.63). The mass spectrometry data were acquired by means of Fourier transform ion cyclotron resonance mass spectrometry (FT-ICR MS). Section 2 provides details on the preparation of the samples and their characterization by elemental and mass spectrometry analyses. Results of the mass attributions and their assignment to probable molecular structures are presented in Section 3. Finally, Section 4 compares these results with the molecular composition and structure of the organic matter of carbonaceous chondrites and with tholins. From these results, we also formulate hypotheses regarding the possible molecular composition of UCAMM organics.

2. SAMPLES AND METHODS

2.1. Production of the Organic Samples. Four chondritic organic matter analogs were synthesized using the Nebulotron (CRPG—CNRS-INSU), a microwave (2.45 GHz) plasma reactor with a vacuum glass chamber in which various gas mixtures can be ionized to produce organic condensates by recombination.[33] The detailed synthesis procedure is described in Kuga *et al.*[48,50] The four Nebulotron samples were prepared from different gas mixtures of CO with N_2 and/or H_2; however, leaks and/or residual amounts of atmospheric components in the reaction chamber have acted as significant sources of N, H, and O (Table S1 of the Supporting Information). For the synthesis of each sample, the main species (CO, N_2, and H_2) were injected in the microwave cavity as a continuous gas flow (of set composition) at a rate of 10 SCCM (Standard Cubic Centimeters per Minute); the estimated temperature of the microwave plasma discharge at 1 mbar was 1000 K. The recombination of the ionization byproducts yields a dark brown solid powder (the organic matter samples of interest) that accumulates in the glass reaction chamber. Aside from these four Nebulotron samples, we also used tholins (aerosol analogs of Titan and Pluto) as an additional benchmark. These tholins were produced from a gas mixture of 95% N_2 and 5% CH_4[54] in the PAMPRE reactor at the LATMOS laboratory.[55−58] After synthesis, all samples were transferred and stored in a glovebox with an argon atmosphere (O_2 < 0.5 ppm). This precaution is mandatory to preserve the integrity of the samples as previous studies have shown that aerosol analogs oxidized in contact with the ambient atmosphere.[59−62] The transfer exposed the organic matter to a regular atmosphere (notably to O_2 and H_2O) for a few minutes. This effect is discussed in Section 4. Throughout these experiments, handling of the samples was done using clean laboratory glassware and stainless steel ware. Powder-free nitrile disposable gloves were used outside the glovebox. Respirators or fume hoods were used to mitigate risks of inhalation when handling tholins since these samples contain nanoparticles. Otherwise, no unexpected or unusual safety hazards were encountered while working with the Nebulotron samples.

2.2. Elemental Analysis. The bulk elemental compositions of the four samples (C, H, N, O, and S elemental content) were measured using a Thermo Scientific FLASH 2000 series CHNS/O Analyzer, equipped with a thermal conductivity detector (TCD). The analysis was performed twice for each sample (between 2 and 5 mg were used for each analysis). The C, H, N, and S percentages were measured after a flash combustion of the sample, generating a gas mixture composed of N_2, CO_2, H_2O, and SO_2, which is eluted through a GC column to be analyzed by the TCD detector. The oxygen percentage is deduced by subtracting the combined percentages of C, H, N, and S from 100%. The accuracy of the resulting values is estimated to be at the percent level.

2.3. Mass Spectrometry. The molecular analyses were performed on a FT-ICR MS Solarix XR from Bruker equipped with a 12 T superconducting magnet from the Infranalytics infrastructure (FR CNRS 2054) at the Rouen node (COBRA, UMR CNRS 6014). By analogy with previous studies on complex organic samples, from natural crude oils and kerogens to synthetic analogs of the atmospheric organics of Saturn's satellite Titan,[54,58] a laser desorption ionization (LDI) source (Nd/YAG × 3 laser at 355 nm) was used to study the samples in the solid state. No separation of the soluble and insoluble fractions was performed. Each powder sample was crushed on a MALDI plate and put under a vacuum for analysis with the following parameters: magnitude mode, plate offset 100 V, deflector plate 200 V, laser shots 100, frequency of laser shots 2000 Hz, funnel 1 at 150 V, and skimmer 1 at 25 V.

External calibration was performed by using tholin samples following the protocol of Maillard *et al.*[54] Tholins and asphaltene references were used for internal calibration for the considered spectral range m/z 100 to 500. Mass spectra were recorded in positive mode with 8 million points and an accumulation of 200 scans (based on the previous works of Maillard *et al.*[54] and Carrasco *et al.*[55]). Detailed resolution values are given in Table S2 of the Supporting Information. Some instrumental parameters, such as the laser power, had to be adjusted to compensate for the variable LDI responses resulting from the molecular differences between the samples.[7,54,63] Consequently, an optimum laser power was determined for each sample in order to obtain similar signal intensities across our analyses and avoid the formation of artifacts at high laser energy. To achieve that, a threshold value

https://doi.org/10.1021/acsearthspacechem.3c00311
ACS Earth Space Chem. XXXX, XXX, XXX−XXX

of 30% of the total signal intensity was selected, *i.e.*, 4% above the beginning of ionization, leading to the best signal-to-noise ratio for each sample (Table S3 and Figure S1 of the Supporting Information). During these trials, MO73 was found to be the hardest to ionize and MO75 the easiest: at a laser power of 25%, the ionization of MO73 was only beginning, while that of MO75 was already complete, leading to the formation of fullerene artifacts.

2.4. Mass Attributions. Calibration was performed on each sample using a minimum of 50 reference ions. Using a quadratic fit, the achieved standard deviation is less than 0.1 ppm at masses of up to m/z 500. Only peaks with a signal/noise ratio above 9 were listed. Molecular formulas were obtained using the SmartFormula tool of the DataAnalysis 6.0 software. For the attributions, both the $[M]^+$ and $[M + H]^+$ ions were considered. The mass error tolerance was set at 0.2 ppm (*e.g.*, an m/z tolerance of $\pm 5 \times 10^{-5}$ at m/z 250). No constraint was set for the lower formula of C, H, O, nor N. On the other hand, to reflect the unique elemental composition of each sample, the upper formulae for N and O were adjusted as follows: MO68: N_{0-14}, O_{0-4}; MO72: N_{0-2}, O_{0-4}; MO73: N_{0-4}, O_{0-4}; MO75: N_{0-6}, O_{0-4}. Only the main isotope of each element (^{12}C, ^{14}N, or ^{16}O) was considered in the attribution process. For each sample, the output of these steps is a list of molecular formulas between m/z 100 and 500 with their associated relative intensity.

To assess the quality of our data processing, we performed analyses of the tholin samples to benchmark and validate our data analysis of the Nebulotron samples. We made a double blind calibration and attribution test, comparing the two different results with Maillard *et al.*[54] with the PyC2MC viewer sofware.[64] We compared the error distributions for the masses, the summed intensities, and the chemical class intensities. We observed the same chemical classes in similar proportions with a good constraint on the error distribution, thus suggesting that our protocol for data analysis was reproducible.

For each sample, the NIST and ChemSpider websites were used to propose representative molecular structures compatible with the general formulas assigned to the 20 most intense peaks within each chemical family (*i.e.*, CH, CHO, CHN, and CHNO).

3. RESULTS

This section describes the information that was retrieved from the FT-ICR data processing, including the mass distribution, chemical families, and possible structures for the main organic molecules present in the samples, keeping in mind that many different isomers might be present for a given m/z value. The last subsection describes the search for m/z values compatible with the presence of molecules of astrobiological interest such as nucleobases and amino acids.

3.1. Elemental Compositions. Results from the elemental analyses of the Nebulotron samples are reported in Table 1 (as elemental ratios relative to C). The elemental compositions of the Nebulotron samples is also compared with a compilation of elemental compositions of the insoluble organic matter (IOM) of carbonaceous chondrites[3] in an elemental ratios plot (H/C versus O/C) diagram showing N/C with a color scale (Figure 1).

Table 1. Elemental Abundances (Relative to C) of the Four Nebulotron Samples

sample	H/C	N/C	O/C
MO68	0.94	0.63	0.53
MO72	0.67	<0.01	0.26
MO73	0.63	0.03	0.24
MO75	0.50	0.16	0.22

Regarding nitrogen, the four Nebulotron samples cover a range of compositions that appear appropriate to evaluate the impact of this element on the structure of early solar organics: two samples present N/C ratios closer to chondritic or solar values (3% for MO73 and 16% for MO75, respectively), while the two others cover more extreme values (<1% for MO72 and 63% for MO68). Regarding the other elements, the MO72, MO73, and MO75 samples also show H/C and O/C ratios close to that of the IOM of carbonaceous chondrites, while the MO68 sample, however, is significantly richer in oxygen. As expected, no sulfur was measured in our samples (no S-bearing species was introduced in the gas mixture nor as any expected contaminant). The elemental analysis of tholins is also reported in Figure 1 since it is used as a reference in this study.

3.2. Molecular Mass Distribution. The mass spectra of the Nebulotron samples (Figure 2) show a large number of signals within the m/z range 100 to 500, which resulted in a similar number of accurate attributions for MO72, MO73, and MO75 (between 1693 and 2733 peaks) despite a difference of an order of magnitude in the observed signal intensities. By contrast, MO68 presented the largest number of attributions (5882) and, as described hereafter, the widest molecular diversity.

We distinguish two contributions in the mass distribution patterns of our samples. The first contribution appears as a broad envelope between m/z values of 100 and (at least) 600 visible on all four spectra. The second contribution corresponds to a pattern of pure carbon molecules detected only in samples MO72, MO73, and MO75 (peaks marked with asterisks in Figure 2). Regarding the broad envelope, the highest intensities are observed at m/z 229.076018 (corresponding to $C_{16}H_9N_2$) for MO75, at m/z 263.085538 (corresponding to $C_{21}H_{11}$) for MO72 and MO73, and at m/z 270.073392 (corresponding to $C_{11}H_8N_7O_2$) for MO68. Regarding the pure carbon molecules, the observed distributions correspond to the molecules C_9–C_{40} for MO72 and MO73, and the molecules C_9–C_{27} for MO75. The peak at m/z 179.999454 (corresponding to C_{15}) in MO73 and MO75 is the most intense of all of their molecules. The FT-ICR MS analysis of the MO75 sample was repeated a second time during a different analytical run (about six months later), but no noticeable differences in the shapes and relative intensities of the two contributions were observed.

While the number of pure carbon species detected is low, their relative intensities exceed those of the main envelope for MO73 and MO75, hinting at their potentially significant abundance in these samples. Based on signal intensity alone, the abundance of these species appears similar for MO73 and MO75, at about twice the intensities observed for MO72. The detailed lists of these peaks are provided in Table 2. Remarkably, the relative intensities of these pure carbon species form a pattern common to the three samples with C_{15} always being responsible for the most intense peak.

3.3. Chemical Families. The almost N-free sample, MO72, is composed of five chemical families: pure C molecules and CH, CHO, CHN, and CHNO species. CH and CHO species are largely dominating, the latter

https://doi.org/10.1021/acsearthspacechem.3c00311
ACS Earth Space Chem. XXXX, XXX, XXX−XXX

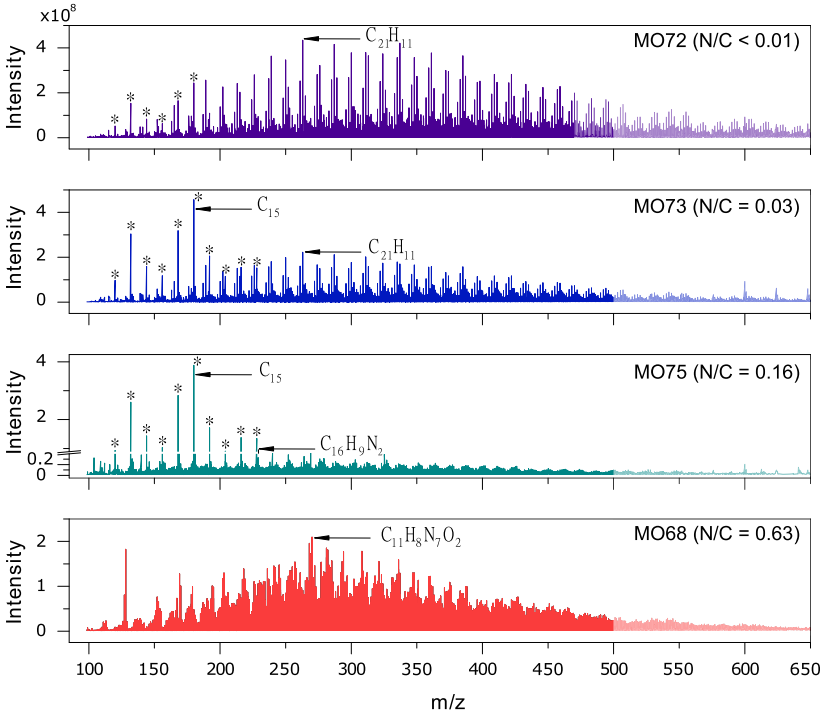

Figure 2. Mass spectra of the four Nebulotron samples obtained from LDI-FT-ICR MS analyses. The nitrogen content of the samples increases from the top plot to the bottom one. The pale section (from m/z 500 to 650) is displayed to show the general shape of the mass pattern, even though the range processed in the present study was limited to m/z 500, due to a lower resolution and higher incertitude in molecular formula assignment obtained above this value. Overall, the spectra of our samples display two components: a broad envelope (visible on all four spectra) and a contribution from pure carbon molecules (visible for MO72, MO73, and MO75). Ions marked with an asterisk correspond to the most intense pure carbon species.

representing 2/3 of the attributions but 1/3 of the total intensity (Figure 3). In the case of the MO73 and MO75 samples, the progressive increase of the nitrogen content results in a decrease of the amount of CH and CHO species in favor of N-bearing species (CHN and CHNO), in terms of both number of attributions and contribution to the total intensity.

The MO68 sample is composed of nearly 99% of N-bearing species, as appears when considering both the raw number of attributions as well as the number of attributions weighted by their respective intensity [scenarios in which CHNO species represent about 70 to 80% of the N-bearing species, respectively (Figure 3)].

3.4. Molecular Structures. For each chemical family (CH, CHO, CHN, and CHNO), we propose in Figure 4 possible hypothetical molecular structures of some of the most intense ions found in each of the four organic analogs. The proposed chemical structures (number of cycles and polycyclic arrangement) can be considered as reliable overall, even though the oxygen and nitrogen atoms as well as the functional groups (ketone and alcohol) may be distributed at different locations on the carbon backbone, since many isomers are statistically likely to exist for each of the selected formula. As the mass spectra maxima are found at m/z between around 230 and 270, and as the largest resolved formulas are up to m/z 500, these molecules are made of no more than a dozen rings.

For the CH family, the more intense peaks in the almost N-free sample (MO72) correspond to highly condensed polycyclic molecules including 6- and 5-membered aromatic or partially unsaturated rings (Figure 4); these molecules include 4 to 9 cycles depending on their molecular weight. For the MO73 sample containing a very small amount of nitrogen (N/C = 0.03), the CH compounds still represent the main chemical family. The molecules are very similar to those of MO72. The polycyclic aromatic hydrocarbons found in MO72 and MO73 are also present in MO75, although at significantly lower abundances. However, some of the CH compounds found in MO75 are slightly different, with linear polyacetylenic chains or with polycyclic molecules including acetylenic substituents or nonplanar PAH/fullerene type molecules with a low number of hydrogen atoms[65] (Figure 4). For MO68, only 9 molecules out of 5882 belong to the CH family.

There are very few CHO species in the most nitrogen-rich samples, MO75 and MO68. In MO72, the most intense peaks of this chemical family correspond to polycyclic molecules containing 19 to 33 carbon atoms and only one oxygen atom. The oxygen is present in either a cyclic ketone or ether, or a hydroxyl group (Figure 4). For the MO73 sample (with a low N/C of 3%), the CHO species ($15 \leq C \leq 29$ and $O = 1$) are very similar in nature.

The CHN family is one of the most abundant groups in the MO73 and MO75 samples. For a lower bulk nitrogen content (MO73), the CHN molecules contain only a low amount of heteroatoms in their chemical formula, with $19 \leq C \leq 30$ and $N = 1$. They correspond to polycyclic structures made of 5- or 6-membered rings, in which the nitrogen atom is most often intracyclic, or to a lesser extent present as a nitrile group. For an intermediate bulk nitrogen content (MO75), the N-bearing molecules are the most intense species after the pure carbon ones. They contain one or two nitrogen atoms for 11 to 24 carbon atoms and consist of polycyclic structures made of three to six 5- or 6-membered rings with intracyclic nitrogen

https://doi.org/10.1021/acsearthspacechem.3c00311
ACS Earth Space Chem. XXXX, XXX, XXX−XXX

Table 2. Table of the Ten Most Intense Ions for Each of the Chemical Families Present in Each Sample[a]

	MO72 (N/C <0.01)		MO73 (N/C = 0.03)		MO75 (N/C = 0.16)		MO68 (N/C = 0.63)	
	Molecular formula	Relative intensity	Molecular formula	Relative intensity	Molecular formula	Relative intensity	Molecular formula	Relative intensity
C	C_{10}	11	C_{10}	20.64	C_{10}	23.28		
	C_{11}	34.79	C_{11}	66.23	C_{11}	66.85		
	C_{12}	18.24	C_{12}	34.36	C_{12}	36.32		
	C_{13}	13.58	C_{13}	25.19	C_{13}	25.85		
	C_{14}	37.4	C_{14}	69.32	C_{14}	72.82	Below detection level	
	C_{15}	55.76	C_{15}	100	C_{15}	100		
	C_{16}	24.39	C_{16}	44.59	C_{16}	43.75		
	C_{17}	13.28	C_{17}	24.49	C_{17}	22.65		
	C_{18}	17.92	C_{18}	33.25	C_{18}	34.87		
	C_{19}	18.88	C_{19}	32.81	C_{19}	34.06		
CH	$C_{19}H_{11}$	83.6	$C_{19}H_{11}$	39.09	C_9H	5.77		
	$C_{21}H_{11}$	100	$C_{20}H_{10}$	43.03	$C_{11}H$	5.27		
	$C_{23}H_{11}$	95.67	$C_{21}H_{11}$	48.25	$C_{11}H_2$	5.39		
	$C_{24}H_{12}$	86.9	$C_{22}H_{10}$	35.84	$C_{12}H_2$	5.56		
	$C_{25}H_{11}$	87.32	$C_{23}H_{11}$	45.67	$C_{13}H$	5.49		
	$C_{25}H_{13}$	83.91	$C_{24}H_{12}$	38.1	$C_{13}H_2$	4.92		
	$C_{26}H_{12}$	85.98	$C_{25}H_{11}$	43.64	$C_{14}H_2$	4.63		
	$C_{27}H_{13}$	96.96	$C_{26}H_{12}$	37.41	$C_{15}H_2$	3.95		
	$C_{29}H_{13}$	86.72	$C_{27}H_{11}$	38.6	$C_{15}H_9$	4.43		
	$C_{31}H_{13}$	83.92	$C_{27}H_{13}$	36.57	$C_{17}H_9$	4.13		
CHO	$C_{19}H_{11}O$	22.17	$C_{16}H_{11}O$	7.11	C_7HO	0.22	$C_{16}H_{14}O_2$	3.27
	$C_{20}H_{13}O$	19.15	$C_{17}H_{11}O$	6.75	C_9HO_2	0.62	$C_{26}H_{16}O_2$	5.06
	$C_{21}H_{11}O$	22.75	$C_{19}H_{11}O$	9.62	$C_{10}HO_2$	0.45	$C_{25}H_{14}O_3$	5.3
	$C_{21}H_{13}O$	19.76	$C_{20}H_{13}O$	7.18	C_9HO_3	0.71	$C_{27}H_{16}O_2$	3.99
	$C_{23}H_{13}O$	23.6	$C_{21}H_{11}O$	10.02	$C_{11}H_3O_2$	0.7	$C_{27}H_{18}O_2$	3.71
	$C_{25}H_{13}O$	24.97	$C_{21}H_{13}O$	7.31	$C_{10}HO_3$	0.66	$C_{30}H_{14}O_3$	2.66
	$C_{26}H_{15}O$	19.26	$C_{23}H_{11}O$	8.05	$C_{12}H_9O$	0.44	$C_{29}H_{16}O_4$	6.02
	$C_{27}H_{13}O$	22.87	$C_{23}H_{13}O$	8.71	$C_9H_3O_4$	0.22	$C_{32}H_{16}O_3$	3.37
	$C_{29}H_{15}O$	19.92	$C_{25}H_{13}O$	8.77	$C_{11}H_3O_3$	0.42	$C_{35}H_{14}O$	2.43
	$C_{33}H_{15}O$	19.65	$C_{27}H_{13}O$	8.37	$C_{12}H_5O_3$	0.25	$C_{32}H_{16}O_4$	3.41
CHN			$C_{20}H_{10}N$	16.03	$C_{11}H_8N$	5.72	$C_3H_7N_6$	37.85
			$C_{21}H_{12}N$	17.34	$C_{12}H_7N_2$	5.78	$C_4H_6N_7$	35.67
			$C_{22}H_{10}N$	14.96	$C_{15}H_{10}N$	5.76	$C_4H_9N_8$	60.68
			$C_{23}H_{12}N$	18.43	$C_{17}H_{10}N$	6.05	$C_6H_9N_{10}$	35.78
			$C_{24}H_{10}N$	15.47	$C_{16}H_9N_2$	7.57	$C_6H_{10}N_{11}$	66.43
			$C_{25}H_{12}N$	15.59	$C_{18}H_9N_2$	6.38	$C_{12}H_8N_7$	33.55
			$C_{26}H_{10}N$	15.83	$C_{20}H_9N_2$	5.88	$C_{12}H_{10}N_7$	33.42
			$C_{26}H_{12}N$	16.15	$C_{20}H_{11}N_2$	6.89	$C_7H_9N_{12}$	61.85
			$C_{28}H_{12}N$	16.26	$C_{22}H_{11}N_2$	6.55	$C_{12}H_9N_8$	35.13
			$C_{30}H_{12}N$	15.62	$C_{24}H_{11}N_2$	6.35	$C_{12}H_{11}N_8$	32.89
CHNO			$C_{16}H_{12}NO$	6.25	$C_{11}H_9N_2O$	3.33	$C_3H_6N_5O$	87.13
			$C_{19}H_{12}NO$	6.83	$C_{10}H_8N_3O$	3.47	$C_{12}H_{10}N_7O$	93.55
			$C_{20}H_{12}NO$	6.09	$C_{13}H_9N_2O$	2.58	$C_{11}H_8N_7O_2$	100
			$C_{20}H_{14}NO$	6.43	$C_{14}H_9N_2O$	3.12	$C_{13}H_9N_6O_2$	88.36
			$C_{21}H_{12}NO$	6.09	$C_{15}H_{11}N_2O$	2.89	$C_{12}H_9N_8O$	78.36
			$C_{22}H_{14}NO$	6.98	$C_{14}H_{10}N_3O$	2.84	$C_{12}H_8N_7O_2$	86.27
			$C_{23}H_{14}NO$	6	$C_{16}H_9N_2O$	2.77	$C_{11}H_9N_8O_2$	74.69
			$C_{24}H_{14}NO$	6.6	$C_{17}H_{11}N_2O$	2.55	$C_{13}H_8N_7O_2$	84.44
			$C_{25}H_{14}NO$	6.64	$C_{16}H_{10}N_3O$	2.76	$C_{14}H_{10}N_7O_2$	85.01
			$C_{27}H_{14}NO$	6.16	$C_{20}H_{11}N_2O$	2.59	$C_{14}H_{10}N_9O_2$	75.78

[a]The most intense ion for each sample is highlighted in yellow (see Table S4 of the Supporting Information for measured masses and associated errors). Gray areas correspond to molecules not considered because of their very low intensities.

atoms (Figure 4). Finally, in the nitrogen-rich MO68 sample, this family is less abundant than the CHNO family. The molecules are made of 5 to 11 nitrogen atoms with 3 to 15 carbon atoms. They consist of polycyclic structures that are less condensed than those in the MO73 and MO75 samples (Figure 4).

The CHNO family is the most abundant in the nitrogen-rich sample MO68. The most intense peaks ($5 \leq N \leq 9$, $3 \leq C \leq 14$, and $1 \leq O \leq 2$) may correspond to polycyclic structures made of one to four 5- or 6-membered rings most often containing from two to four nitrogen atoms (typically triazole, tetrazole...). In these possible structures, the oxygen atoms are very often present as ketone or intracyclic ether. Moreover, it is important to note that the molecules present in MO68 are far less condensed than those present in the three other samples. They also display a very rich chemical diversity resulting from the larger number of heteroatoms (mainly nitrogen atoms) present in the molecular structures. In the MO73 sample (N/C = 0.03), there is only one nitrogen and one oxygen in the CHNO molecules ($15 \leq C \leq 32$). As for the CHN compounds, the molecules have condensed aromatic structures wherein nitrogen and oxygen are most often intracyclic or

https://doi.org/10.1021/acsearthspacechem.3c00311
ACS Earth Space Chem. XXXX, XXX, XXX−XXX

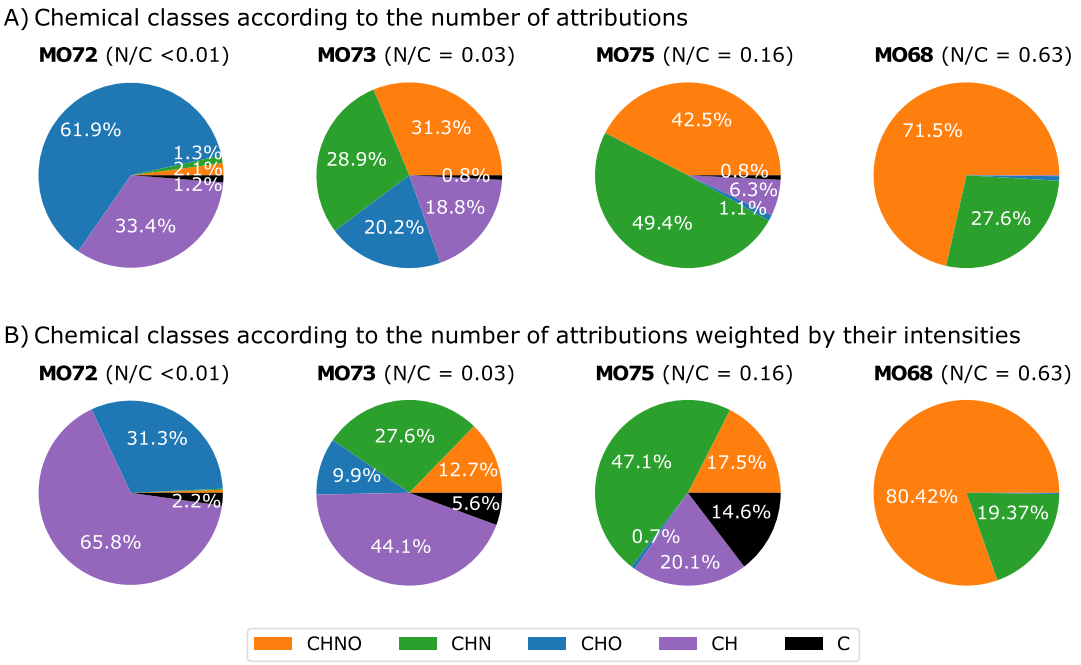

Figure 3. Evolution of the relative amount of chemical classes in the Nebulotron samples as a function of their N/C ratios (N/C increasing from left to right).

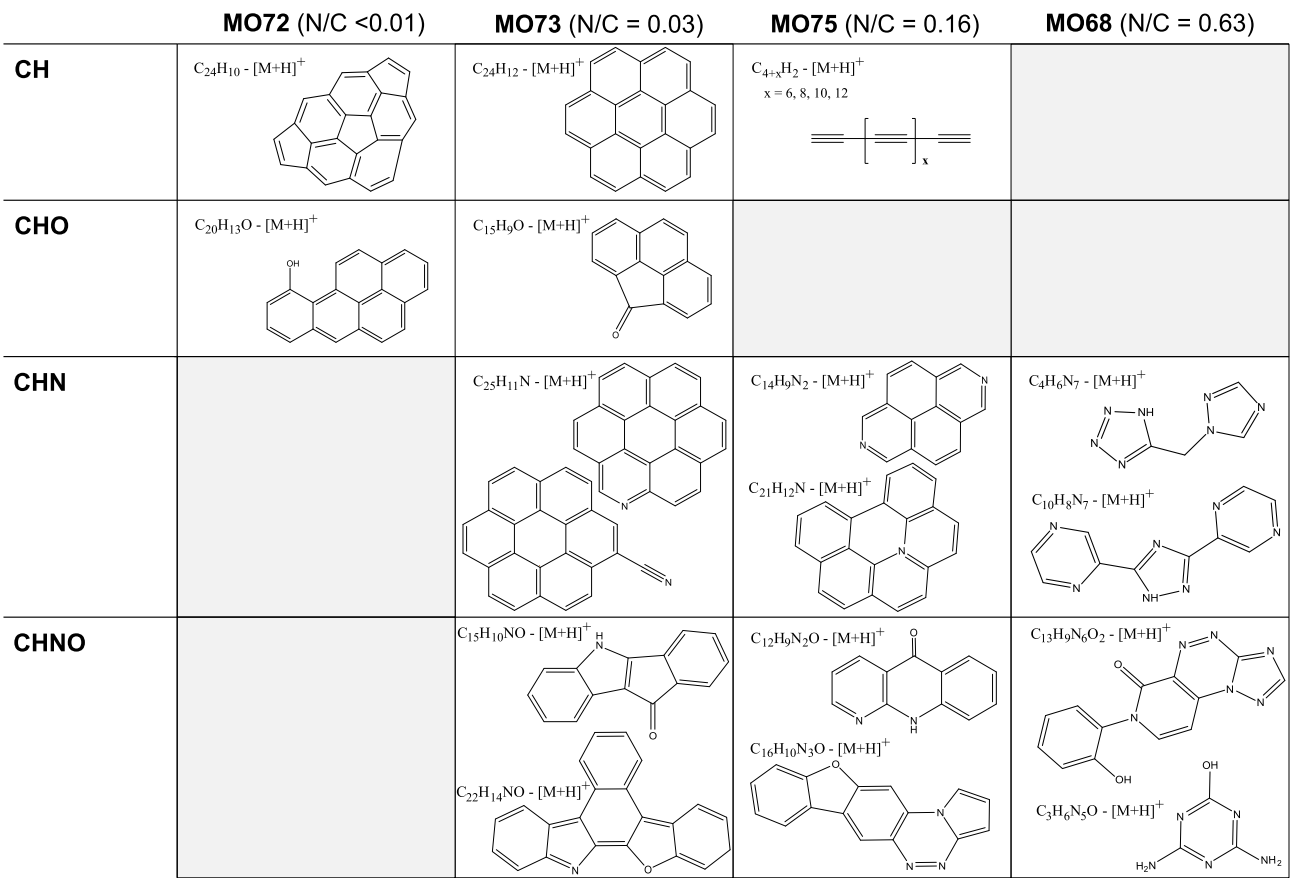

Figure 4. Possible representative molecular structures of the most abundant CH, CHO, CHN, and CHNO compounds found in the four Nebulotron samples. $C_{24}H_{12}$ and $C_{24}H_{10}$ have been identified in MO72 and MO73 as possible nonplanar polyaromatics and $C_{4+x}H_2$ in MO75. $C_{20}H_{13}O$ has been identified in MO72 and MO73 and $C_{15}H_9O$ in MO73. Additional possible structures are presented in the following figures of the Supporting Information: Figure S2 for CH compounds, Figure S3 for CHN compounds, and Figure S4 for CHNO compounds. Gray areas correspond to molecules that were not considered because of their very low intensities.

https://doi.org/10.1021/acsearthspacechem.3c00311
ACS Earth Space Chem. XXXX, XXX, XXX−XXX

present as ketone (Figure 4). In MO75, which contains more nitrogen (N/C = 0.16), the number of nitrogen atoms is larger with typically two to three atoms per molecule ($9 \leq C \leq 22$) while there is only one oxygen atom. The molecules are very similar to those of the CHN family, with the addition of an oxygen atom present in the structure as a cyclic ketone or ether.

In summary, most of the molecules identified in our samples appear to be condensed aromatics. In the N-bearing families (CHN and CHNO), however, the presence of heteroatoms results in fewer condensed molecules. This may have implications for their stability, as discussed in Section 4.

3.5. Potential Presence of Molecules of Astrobiological Interest. The origin of the biochemical mechanisms permitting life and their evolution from prebiotic chemistry remain unknown. The presence in prebiotic environments of the organic molecules used by terrestrial life thus holds much interest in our attempt to decipher the origin of life. These "molecules of astrobiological interest" notably include nucleobases and amino acids formed through abiotic mechanisms. Molecular formulas assigned to some of the m/z values present in the FT-ICR MS spectra of our samples are compatible with the presence of such molecules (Table 3). However, as mentioned before, each resolved molecular formula could correspond to many isomers, which may or may not be related to the molecules of interest. The FT-ICR MS technique behind our data does not lead to the fragmentation of the sample molecules and thus offers no path to discriminate between isomers; consequently, it should be kept in mind that our resolved formulas are not conclusive proof of the presence of specific molecules in our samples. Nevertheless, molecules of astrobiological interest were previously identified within Nebulotron analogs and early stage carbonaceous meteorites.[23] Molecular formulas resolved from our samples are compatible with nucleobases constitutive of DNA and RNA and with some of their derivatives. Among the set of amino acids utilized by life, m/z values compatible with histidine, phenylalanine, and tryptophan were detected in our Nebulotron samples with higher nitrogen contents (MO75 and MO68) (Table 3). Similarly, m/z values compatible with the canonical nucleobases found in DNA and RNA (cytosine, uracil, thymine, adenine, and guanine) were also observed. The possible presence of glycine and alanine cannot be assessed from our data since their molecular masses fall below the detection range of the 12 T FT-ICR mass spectrometer as it was configured for our analyses.

The amount of molecules of astrobiological interest in our samples remains very small, even when considering the most favorable case in which the entire signal at a given m/z would result only from the isomer of interest (and not any other isomer). Using the intensity of the peaks as a proxy to their relative amount, we find that these molecules represent 0.11 and 0.06% of the total amount of molecules of MO75 and MO68, respectively. This amount has implications for calculating the quantity of material that needs to be collected by future space missions, such as a mission through the Enceladus geysers and the Dragonfly mission to Titan, in order to detect the presence of such molecules.

Table 3. Molecular Formula Identified in the Nebulotron Samples and Compatible with the Presence of Molecules of Astrobiological Interest[c]

molecules of astrobiological interest	molecular formula	measured mass $[M + H]^+$	error (ppm)	relative intensity
histidine[a]	$C_6H_9N_3O_2$			
MO75		156.07675	0	0.35
MO68		156.076784	−0.2	1.38
phenylalanine[a]	$C_9H_{11}NO_2$			
MO75		166.086258	0	0.35
MO68				
tryptophan[a]	$C_{11}H_{12}N_2O_2$			
MO75		205.097165	−0.1	0.78
MO68		205.097163	0	1.26
cytosine[b]	$C_4H_5N_3O$			
MO75		112.050542	0	1.06
MO68		112.050531	0.06	5.04
uracil[b]	$C_4H_4N_2O_2$			
MO75		113.03456	−0.05	0.83
MO68		113.034549	0	1.3
thymine[b]	$C_5H_6N_2O_2$			
MO75		127.0502	0.04	0.76
MO68		127.050198	0	1.67
adenine[b]	$C_5H_5N_5$			
MO75		136.061779	−0.1	0.65
MO68		136.061775	−0.1	13.55
guanine[b]	$C_5H_5N_5O$			
MO75		152.056686	0	1.21
MO68		152.056696	−0.06	32.45

[a]Amino acids. [b]Nucleobases. [c]Intensities are given relative to the most intense peak of each sample.

4. DISCUSSION

4.1. Effect of Nitrogen on the Structure. One objective of this study is to investigate the effect of the N/C ratio on the molecular structure of the Nebulotron samples. Figure 5 illustrates how quickly the number of N-bearing molecules increases in Nebulotron samples with higher N/C ratios. The rapidly increasing fraction of N-bearing species and the increasing prominence of the CHN and CHNO families suggest a relatively homogeneous repartition of the nitrogen in the molecular structure of the samples.

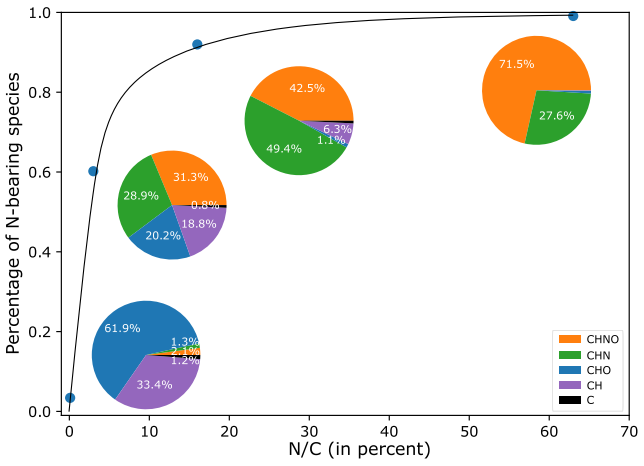

Figure 5. Evolution of the fraction of N-bearing species and evolution of the relative proportions of the chemical families (C, CH, CHO, CHN, and CHNO) identified in the Nebulotron samples as a function their N/C ratio.

https://doi.org/10.1021/acsearthspacechem.3c00311
ACS Earth Space Chem. XXXX, XXX, XXX−XXX

Table 4. Chemical Sub-Families Identified in Nebulotron Samples for O- and/or N-Bearing Molecules with a Peak Intensity above 0.5% of the Maximum Peak Intensity

	MO72 (N/C < 0.01)	MO73 (N/C = 0.03)	MO75 (N/C = 0.16)	MO68 (N/C = 0.63)
O-containing subfamilies $C_xH_yO_i$	4 with i = 1−4	3 with i = 1−3	very low amount	very low amount
N-containing subfamilies $C_xH_yN_j$	very low amount	2 with$j$ = 1−2	4 with j = 1−5	10 with j = 3−15
N- and O-containing subfamilies $C_xH_yN_jO_i$	very low amount	4 with j = 1−2, i = 1−3	13 with j = 1−5, i = 1−3	41 with j = 3−13, i = 1−4

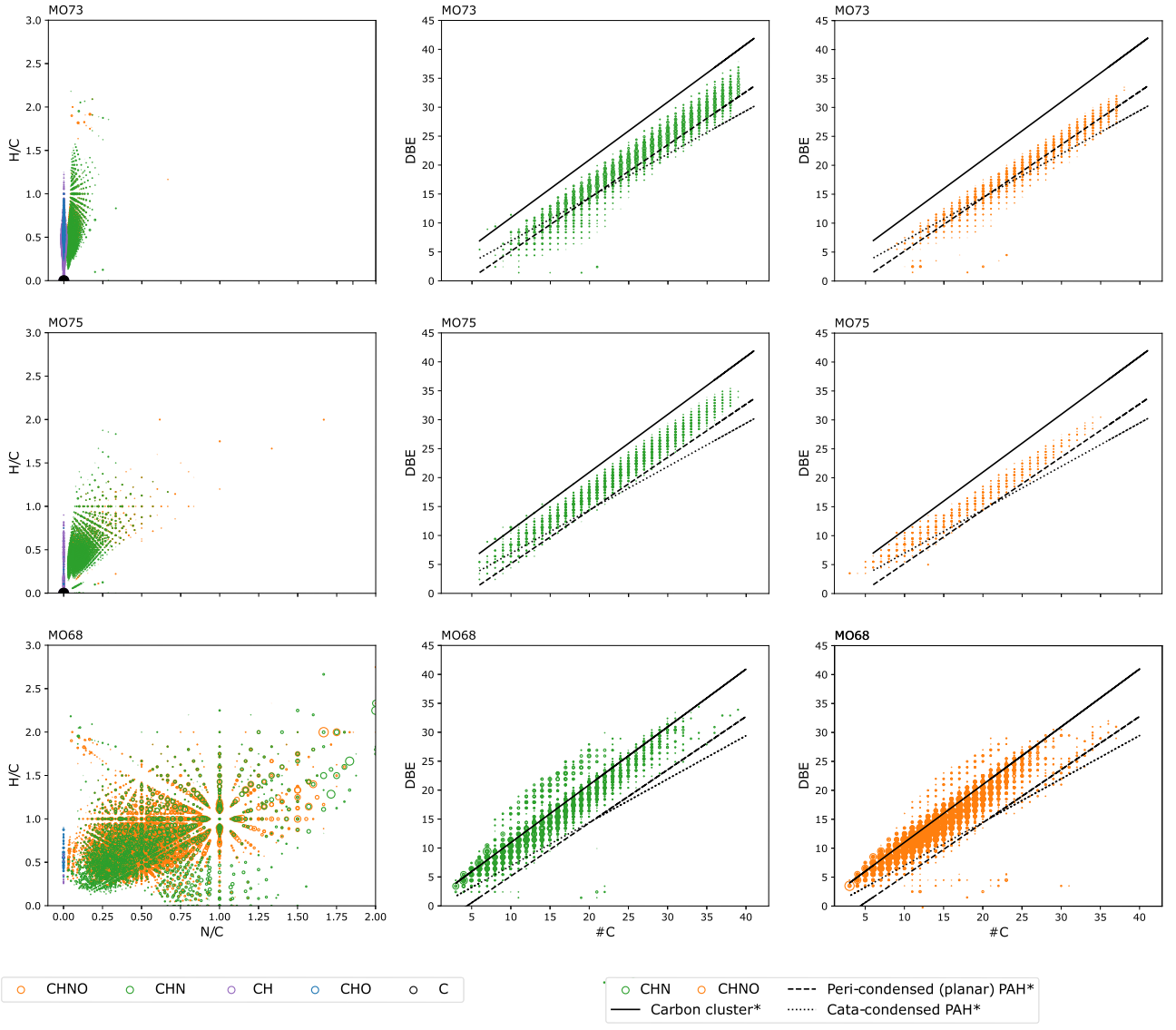

Figure 6. Elemental ratio plots of H/C versus N/C (left column) and DBE versus carbon number (#C) of CHN compounds (middle column) and CHNO compounds (right column) for the samples MO73 (top line), MO75 (middle line), and MO68 (bottom line). In the DBE plots, the lines of carbon cluster, peri-condensed PAH, and cata-condensed PAH have been computed using the equations from Joshi *et al.*;[65] their equations are DBE = C + 1 (solid lines), DBE = 0.92 × C − 4 (dashed lines), and DBE = 0.75 × C − 0.5 (dotted lines), respectively.

We also observe a gradual increase of the chemical diversity in terms of number of subfamilies of heteroatom-containing products, that is, in terms of number of chemical formula with a given number of oxygen and/or nitrogen atoms and a variable number of carbon and hydrogen atoms (see Table 4). For example, four main subfamilies (*i.e.*, chemical formulas) of N- and O-containing products are detected in the MO73 sample ($C_xH_yN_jO_i$, with j = 1−2 and i = 1−3), while in the sample showing the highest nitrogen content (MO68), 41 different CHNO subfamilies could be identified. However, a precise quantitative assessment of the relative amount of each subfamily within the samples is not possible since the response to ionization (*i.e.*, the individual peak intensity) significantly differs between molecules, in particular as a function of the heteroatoms present in their chemical formula (CH versus CHO versus CHN versus CHNO).

Another effect of the nitrogen content is to increase the number of unsaturated bonds as measured by the double bond equivalent (DBE) number. The DBE is obtained with the following formula

$$\mathrm{DBE} = (2 \times \mathrm{C} - \mathrm{H} + \mathrm{N} + 2)/2$$

https://doi.org/10.1021/acsearthspacechem.3c00311
ACS Earth Space Chem. XXXX, XXX, XXX−XXX

Table 5. Comparison of the Composition of the Nebulotron Samples (this study) with the IOM of the Paris Meteorite (data from Danger *et al.* (2020)[66])[c]

	MO72 (N/C < 0.01)	MO73 (N/C = 0.03)	MO75 (N/C = 0.16)	MO68 (N/C = 0.63)	Paris IOM (N/C = 0.04)[44]
C	21 (1.2%)	22 (0.8%)	19 (0.8%)	0	45 (<0.5%)
CH	552 (33.4%)	495 (18.8%)	132 (6.3%)	9 (<0.5%)	1577 (11.4%)
CHO	1061 (61.0%)	557 (20.2%)	26 (1.1%)	47 (<1%)	2091 (15.2%)
CHN	23 (1.3%)	797 (28.9%)	1190 (49.4%)	1621 (25.6%)	4626 (33.6%)
CHNO	36 (2.1%)	862 (31.3%)	1023 (42.5%)	4205 (71.5%)	5447 (39.5%)
all N-bearing molecules	59 (3.4%)	1659 (61%)	2213 (93%)	5826 (99%)	10,073[a] (73%)
total	1693	2733	2390	5882	13,786[a]
aliphatics	49	27	29	183	280
aromatics	52	74	140	523	952
condensed aromatics	1592 (94%)	2632 (96%)	2221 (93%)	5176 (88%)	20,626 (94%)
total	1693	2733	2390	5882	21,881[b]

[a]Unlike the Nebulotron samples, the Paris IOM contains S-bearing molecules. In order to offer a more direct comparison of the relative proportions of the C, CH, CHO, CHN, and CHNO families between the Paris IOM and Nebulotron samples, these S-bearing molecules have been excluded from the first total counts of molecules. [b]The S-bearing molecules are included in the second total count of molecules, as these molecules are included in the aliphatics, aromatics, and condensed aromatics counts given for the Paris IOM in Danger *et al.*[66] [c]N/C value given for the IOM of the Paris meteorite corresponds to the bulk elemental analysis conducted by Vinogradoff *et al.* (2017).[44]

with higher DBE values indicating a higher degree of unsaturation. The DBE is plotted against the carbon number (#C) in Figure 6 for the CHN family (middle column) and CHNO family (right column). As the samples are enriched with nitrogen, the DBE value becomes larger. Many attributions are above the so-called "impossible mass" domain established for molecules that contain C and H atoms only,[65] which is due to the large number of nitrogen atoms.

When considering the molecular structures likely present within the CHN family (Figure 4), similar highly condensed polycyclic aromatic hydrocarbons are observed for MO73 and MO75, containing one or two (MO75) N-heterocycles. By contrast, in the case of MO68, less condensed structures are observed. They consist of chains of 5- and 6-membered unsaturated heterocycles containing up to three or four nitrogen atoms. The same trend is observed within the CHNO family (Figure 4). Nitrogen atoms are present in most of the molecules as evidenced by the gradual increase of the proportions of the CHN and CHNO families (MO73 and MO75) to end up with a composition dominated by CHNO species in MO68 (Figure 3). The N/O atomic ratio is high (about 3 to 8) in this nitrogen-rich sample. It is worth noting that the O and N atoms in most of the compounds are present in rings and to a lower extent in extra-cyclic functional groups such as ketones, nitrile, or alcohols (Figure 4), which is in agreement with spectroscopic observations made by Kuga *et al.*[48] As mentioned above, a brief atmospheric exposure may result in a partial oxidation of the samples during their transfer from the synthesis chamber to their storage under argon. This oxidation may be responsible for the addition of extra-cyclic functional groups ketones and alcohols. This is further evidenced by the similarity between the CH and CHO structures. The significant difference in composition between MO73 and MO75 versus MO68 suggests that MO68 would have a higher chemical reactivity; in the presence of liquid water under temperature and pressure conditions mimicking those present inside the larger icy worlds of the solar system (the larger icy moons and dwarf planets), nitrogen-rich organics may react more easily with dissolved ions and form volatile species and complex residual organics.

4.2. Comparison with the IOM Fraction of the Paris Meteorite. Organics in meteorites have been analyzed with LDI-FT-ICR MS, but only a few studies have provided details on their constituting chemical families. As detailed later in this subsection, when compared with the IOM isolated from the Paris meteorite (one of the least altered CM chondrites known),[66] we find an excellent match between the chemical makeup of this IOM and those of our MO73 and MO75 samples, which is consistent with their similar N/C ratios (0.04 for the IOM).[44] From our data, Table 5 compiles, for each Nebulotron sample, the absolute number of molecular formulas (and the relative proportion to total) corresponding to each chemical family (C, CH, CHO, CHN, and CHNO). Table 5 also includes similar data reported by Danger *et al.* (2020) for the Paris meteorite IOM.[66] Although both data sets were acquired using the same analytical technique and instrument, we note that our analyses have been made on the bulk Nebulotron samples, which likely included a small fraction of soluble organics, unlike the Paris meteorite IOM analyzed by Danger *et al.*[66] Furthermore, unlike the Nebulotron samples, the Paris IOM contains S-bearing molecules; thus, in order to offer a more direct comparison of the relative proportions of the C, CH, CHO, CHN, and CHNO families between the Paris IOM and Nebulotron samples, S-bearing molecules have been excluded from the first total counts of molecules given for the Paris IOM (total counts marked with an "a" in Table 5), so that all non-S-bearing chemical families amount to 100%.

The number of attributions in the present study is significantly lower by comparison with the analysis of the Paris meteorite IOM by Danger *et al.*: even after subtraction of the S-bearing molecules, Danger *et al.* still have more than twice our number of attributions.[66] This can be explained by our choice of narrower/stricter values for several parameters of the data processing, notably, (i) a signal-to-noise ratio (S/N) of 9 (compared to 6 in Danger *et al.*[66]), (ii) a limit of ±0.2 ppm (versus 0.4 ppm) for the formula attribution, and (iii) a 0.1 ppm standard deviation (versus 0.2 ppm) used for the calibration. Furthermore, Danger *et al.*[66] considered mass ranges up to m/z 700, whereas an m/z limit of 500 was selected in our work to be consistent with our calibration. We do not think that the laser power contributed significantly to this difference because we used the same empirical rule related to the formation of fullerenes by ionization of the samples (see

https://doi.org/10.1021/acsearthspacechem.3c00311
ACS Earth Space Chem. XXXX, XXX, XXX−XXX

Figure S1 of the Supporting Information). In addition, the larger number of molecules in the Paris meteorite IOM is related to a smaller number of heteroatoms per molecule.

In more detail, we may compare the fraction that each chemical family represents relative to the total number of molecules resolved in our Nebulotron samples and in the Paris meteorite IOM (again, excluding S-bearing molecules for the latter). The CH family corresponds to 11.4% of the molecules identified in the Paris meteorite IOM. This value lies between those of 6.3% for MO75 and 18.8% for MO73. For the CHO family, the percentage in the Paris IOM (15.2%) also lies between the values for MO73 (20.2%) and MO75 (1.1%). The same observation can be made for the CHN family (33.6% for the Paris IOM, between 28.9% for MO73 and 49.4% for MO75) and for the CHNO family (39.5% for the Paris IOM, between 31.3% for MO73 and 42.5% for MO75). Pure carbon molecules are present in both the Paris meteorite IOM and our Nebulotron samples. Interestingly, their fractions in each sample appear similarly small, with 0.5% for the Paris IOM and 0.8% for MO73 and MO75. It has been suggested by Kuga that graphite-type carbon molecules could form from the pyrolysis/carbonization process taking place in the Nebulotron.[68] However, the comparison with the Paris IOM suggests that this process could also take place during the formation of the primordial IOM in the early solar system. In any case, this remains a very small fraction of the carbonaceous material.

Further comparisons can be established by applying the Danger *et al.* definitions of aliphatics, aromatics, and condensed aromatics to our samples.[66] These definitions are based on a value of X_c defined as

$$X_c = ((2 \times C + N - H - 2 \times m \times O) / (DBE - m \times O))$$

where DBE = $(2 \times C - H + N + 2)/2$, and $m = 0.75$ is the estimated fraction of oxygen double bonds.[44,66,67] Danger *et al.*[66] defined aliphatics with $0 < X_c < 2.5$, aromatics with $2.5 < X_c < 2.7$, and condensed aromatics with $X_c > 2.7$. The resulting values for our samples are compared in Table 5 to the values calculated for the Paris IOM by Danger *et al.*[66] Note that for the Paris IOM, these values encompass all resolved molecular formulas, which includes the S-bearing ones (total count marked with a "b" in Table 5). Using these definitions, 94% of the molecules in the Paris meteorite IOM were found to be condensed aromatics, a value once again bracketed by those of our samples MO75 (93%) and MO73 (96%).

Overall, this detailed comparison with the Paris meteorite IOM (elemental ratios, relative proportions of chemical families, and abundances of aromatics and aliphatics) suggests that the Nebulotron samples with intermediate N/C (MO73 and MO75) constitute good analogs of the organic matter isolated from primitive carbonaceous chondrites.

The ultracarbonaceous Antarctica micrometeorites (UCAMMs) constitute a class of meteorites significantly enriched in nitrogen (Figure 1) compared to carbonaceous chondrites. Their N/C ratio can reach values of up to 20%,[12] closer (compared to carbonaceous chondrites) to the solar value of 24%.[51] However, no FT-ICR analysis has yet been performed on these minute samples, which prevents any detailed comparison with our samples richer in nitrogen (and any conclusive assessment of the quality of the N-rich Nebulotron samples as analogs to UCAMMs). Nonetheless, hypotheses regarding UCAMMs may be proposed from our results. Most notably, our analyses show very clearly how higher N/C ratios lead to a dramatic increase in the incorporation of nitrogen in most of the constitutive molecules of the Nebulotron samples; for a N/C value of about 0.2, more than 90% of FT-ICR resolvable formulas contain nitrogen (Figure 5). This "homogeneous distribution" of nitrogen is supported by the analysis of tholins (see Section 4.3 hereafter), whose high N/C ratio (about 0.5) leads to an overwhelming majority (99%) of N-bearing molecules. From these combined observations, we predict that most organic molecules in UCAMMs could be N-bearing compounds, and that overall, these molecules should be richer in heteroatoms and less condensed than the organic molecules found in carbonaceous chondrites. This hypothesis should be tested whenever high-resolution mass spectrometry data are acquired from UCAMMs organics, notably to determine if the widespread incorporation of nitrogen in primitive organics holds as a general rule or reveals itself as a specificity of only some organics synthesis pathways.

4.3. Comparison with Tholins. Titan, Saturn's largest moon, is the only moon in the solar system with a dense atmosphere (about 1.5 bar at Titan's surface) made essentially of N_2 and with a few percent of CH_4. In Titan's upper atmosphere, organics are produced by the photolysis of methane and nitrogen.[69] This process is responsible for the formation of an organic haze that falls on the surface and eventually accumulates in dunes that will be analyzed by the Dragonfly mission.[70] Analogs of Titan's organic haze are produced in laboratories and known as tholins.[52] These organic analogs have been previously analyzed with FT-ICR MS.[61,63] Since tholins contain a lot of nitrogen but very little oxygen, more than 99% of their constitutive molecules contain nitrogen. In their m/z versus H/C plots, Maillard *et al.* (2018) found that lighter organic molecules form a soluble part with a H/C ratio peaking at 1.5 and a N/C ratio peaking at 0.5.[54] The insoluble organics have a similar N/C ratio but a much smaller H/C ratio peaking at 0.75,[54] a value close to that of the Nebulotron samples of the present study. By comparison, our elemental analysis of the PAMPRE tholins used in our study led to an N/C ratio of 0.62 and an H/C ratio of 1.16 (Figure 1). The molecules of the soluble fraction belong to the pyrazole and triazine families.

As we performed analysis of these tholins to benchmark our analysis process, we also investigated how nitrogen is integrated within their molecular structure. Among our samples, MO68 is the one with the largest N/C ratio. Although this sample contains much more oxygen (comparatively to the tholins) due to the presence of CO during its synthesis, we found that 99% of its constitutive molecules include nitrogen, mostly present in 5- and 6-membered aromatic or partially unsaturated rings, resulting in an increase of the unsaturation degree also observed in tholins (Figure 4). Even aromatics formed with less nitrogen (*e.g.*, as in the MO75 sample) are rich in nitrogen-based heterocycles (Figure 4). The present study also shows that for the nitrogen-rich samples, less condensed polycyclic molecules are obtained. This is consistent with the finding that tholins would be composed of small aromatic cores linked together with short chains.[71] Identifying these common structures in N-rich samples hint at a more systematic structuration/configuration that may be found in different astrochemical contexts in which organics are produced through the photodissociation of H−C−N−O-bearing volatiles.

https://doi.org/10.1021/acsearthspacechem.3c00311
ACS Earth Space Chem. XXXX, XXX, XXX−XXX

5. CONCLUSIONS

We have assessed and compared the molecular makeup of four synthetic analogs of primordial organic material produced by photodissociation of C−H−N−O volatiles in a plasma reactor (the Nebulotron experiment). The four samples are characterized by nitrogen contents ranging from N/C < 0.01 to N/C = 0.63, a set of compositions bracketing the N/C values of carbonaceous chondrites, of ultracarbonaceous micrometeorites, and the solar N/C value. FT-ICR MS analyses have revealed that samples with a higher N/C ratio exhibit a greater fraction of N-bearing molecules. In our synthetic samples, nitrogen is often present with oxygen as part of 5- and 6-membered rings or as functional groups (cyclic ketone, alcohol, or amine). The molecular composition and structure of the organic molecules isolated from the Paris chondrite IOM (N/C = 0.04) are close to those of our analogs with bracketing nitrogen contents of 3% (MO73) and 16% (MO75). This confirms that Nebulotron samples are relevant analogs of chondritic IOM. Molecules of prebiotic interest may be present in the Nebulotron samples containing a significant amount of nitrogen. The intensity, and therefore the fraction, of these molecules is, however, quite small in the analogs with N/C ratios closer to the chondritic values. Confirmation of the presence of such molecules in natural samples would thus require the use of separation techniques such as liquid chromatography coupled to high-resolution mass spectrometry. In recent studies, various quantities of IOM have been proposed to explain the low density of the refractory cores of Ganymede and Titan.[72,73] Based on our results, Nebulotron samples could represent an attractive starting material for laboratory experiments assessing the fate of the primordial organic matter during the accretion, differentiation, and later evolution of the icy bodies of the solar system and beyond.

■ ASSOCIATED CONTENT

Supporting Information

The Supporting Information is available free of charge at https://pubs.acs.org/doi/10.1021/acsearthspacechem.3c00311.

DOI link to the DataAnalysis process parameters and output (resolved formulas with relative intensities) for all samples of this study, gas mixture compositions used in the Nebulotron plasma chamber to synthesize the four Nebulotron samples, FT-ICR peaks resolution for the four samples of this study, laser power used for the FT-ICR analyses, expanded version of Table 2 with the most intense masses detected in the four samples of this study, response of each sample to increasing laser power used to determine the optimal laser power for the FT-ICR analyses, and expanded versions of Figure 4 with probable molecular structures for the most intense peaks/formulas seen in the CH, CHN, and CHNO families (PDF)

■ AUTHOR INFORMATION

Corresponding Authors

Pauline Lévêque − *Nantes Université, Univ. Angers, Le Mans Université, CNRS, Laboratoire de Planétologie et Géosciences, LPG UMR 6112, Nantes 44000, France; CEISAM, Nantes Université, UMR-CNRS 6230, Nantes F-44000, France;* orcid.org/0009-0004-6697-9570; Email: pauline.leveque@univ-nantes.fr

Christophe Sotin − *Nantes Université, Univ. Angers, Le Mans Université, CNRS, Laboratoire de Planétologie et Géosciences, LPG UMR 6112, Nantes 44000, France;* Email: christophe.sotin@univ-nantes.fr

Authors

Clémence Queffelec − *CEISAM, Nantes Université, UMR-CNRS 6230, Nantes F-44000, France;* orcid.org/0000-0001-9794-7441

Carlos Afonso − *Normandie Université, COBRA, UMR 6014, FR 3038, Université de Rouen, INSA de Rouen-Normandie, CNRS, IRCOF, Mont Saint Aignan 76821, France;* orcid.org/0000-0002-2406-5664

Olivier Bollengier − *Nantes Université, Univ. Angers, Le Mans Université, CNRS, Laboratoire de Planétologie et Géosciences, LPG UMR 6112, Nantes 44000, France*

Adriana Clouet − *Nantes Université, Univ. Angers, Le Mans Université, CNRS, Laboratoire de Planétologie et Géosciences, LPG UMR 6112, Nantes 44000, France*

Erwan Le Menn − *Nantes Université, Univ. Angers, Le Mans Université, CNRS, Laboratoire de Planétologie et Géosciences, LPG UMR 6112, Nantes 44000, France*

Yves Marrocchi − *Centre de Recherches Pétrographiques et Géochimiques, UMR 7358 CNRS-Université de Lorraine, Vandoeuvre-lès-Nancy F-54501, France*

Isabelle Schmitz − *Normandie Université, COBRA, UMR 6014, FR 3038, Université de Rouen, INSA de Rouen-Normandie, CNRS, IRCOF, Mont Saint Aignan 76821, France;* orcid.org/0000-0003-0665-0074

Bruno Bujoli − *CEISAM, Nantes Université, UMR-CNRS 6230, Nantes F-44000, France*

Complete contact information is available at: https://pubs.acs.org/10.1021/acsearthspacechem.3c00311

Notes

The authors declare no competing financial interest.

■ ACKNOWLEDGMENTS

P.L. acknowledges support by the CNRS-PRIME 80 program. This work has been funded by the European Union (ERC, PROMISES, project #101054470). Views and opinions expressed are, however, those of the authors only and do not necessarily reflect those of the European Union or the European Research Council. Neither the European Union nor the granting authority can be held responsible for them. The authors thank Laurent Tissandier (CRPG Nancy, France) for preparing the organic samples with the Nebulotron instrument. The authors also thank Thomas Gautier and Zoé Perrin (LATMOS Guyancourt, France) for preparing the tholin samples with the PAMPRE instrument. Access to the CNRS research infrastructure Infranalytics (FR2054) is gratefully acknowledged. Denis Loquet is greatly acknowledged for his help in recording the elemental analyses. We thank the reviewers for their insightful comments, which improved the manuscript.

■ REFERENCES

(1) Lodders, K. Solar System Abundances and Condensation Temperatures of the Elements. *Astrophys. J.* **2003**, *591* (2), 1220−1247.

(2) Pearson, V. K.; Sephton, M. A.; Franchi, I. A.; Gibson, J. M.; Gilmour, I. Carbon and Nitrogen in Carbonaceous Chondrites:

Elemental Abundances and Stable Isotopic Compositions. *Meteorit. Planet. Sci.* **2006**, *41* (12), 1899−1918.
(3) Alexander, C. M. O.; Fogel, M.; Yabuta, H.; Cody, G. D. The Origin and Evolution of Chondrites Recorded in the Elemental and Isotopic Compositions of Their Macromolecular Organic Matter. *Geochim. Cosmochim. Acta* **2007**, *71* (17), 4380−4403.
(4) Derenne, S.; Robert, F. Model of Molecular Structure of the Insoluble Organic Matter Isolated from Murchison Meteorite. *Meteorit. Planet. Sci.* **2010**, *45* (9), 1461−1475.
(5) Schmitt-Kopplin, P.; Gabelica, Z.; Gougeon, R. D.; Fekete, A.; Kanawati, B.; Harir, M.; Gebefuegi, I.; Eckel, G.; Hertkorn, N. High Molecular Diversity of Extraterrestrial Organic Matter in Murchison Meteorite Revealed 40 Years after Its Fall. *Proc. Natl. Acad. Sci. U.S.A.* **2010**, *107* (7), 2763−2768.
(6) Schmitt-Kopplin, P.; Harir, M.; Kanawati, B.; Tziozis, D.; Hertkorn, N.; Gabelica, Z. Chemical Footprint of the Solvent Soluble Extraterrestrial Organic Matter Occluded in Sołtmany Ordinary Chondrite. *Meteorites* **2012**, *2* (1−2), 79−92.
(7) Laurent, B.; Maillard, J.; Afonso, C.; Danger, G.; Giusti, P.; Remusat, L. Diversity of Chondritic Organic Matter Probed by Ultra-High Resolution Mass Spectrometry. *Geochem. Perspect. Lett.* **2022**, *22*, 31−35.
(8) Alexander, C. M. O.; Newsome, S. D.; Fogel, M. L.; Nittler, L. R.; Busemann, H.; Cody, G. D. Deuterium Enrichments in Chondritic Macromolecular Material—Implications for the Origin and Evolution of Organics, Water and Asteroids. *Geochim. Cosmochim. Acta* **2010**, *74* (15), 4417−4437.
(9) Piani, L.; Robert, F.; Beyssac, O.; Binet, L.; Bourot-Denise, M.; Derenne, S.; Le Guillou, C.; Marrocchi, Y.; Mostefaoui, S.; Rouzaud, J.-N.; Thomen, A. Structure, Composition, and Location of Organic Matter in the Enstatite Chondrite Sahara 97096 (EH3). *Meteorit. Planet. Sci.* **2012**, *47* (1), 8−29.
(10) Duprat, J.; Dobrică, E.; Engrand, C.; Aléon, J.; Marrocchi, Y.; Mostefaoui, S.; Meibom, A.; Leroux, H.; Rouzaud, J.-N.; Gounelle, M.; Robert, F. Extreme Deuterium Excesses in Ultracarbonaceous Micrometeorites from Central Antarctic Snow. *Science* **2010**, *328* (5979), 742−745.
(11) Dartois, E.; Engrand, C.; Brunetto, R.; Duprat, J.; Pino, T.; Quirico, E.; Remusat, L.; Bardin, N.; Briani, G.; Mostefaoui, S.; Morinaud, G.; Crane, B.; Szwec, N.; Delauche, L.; Jamme, F.; Sandt, Ch.; Dumas, P. UltraCarbonaceous Antarctic Micrometeorites, Probing the Solar System beyond the Nitrogen Snow-Line. *Icarus* **2013**, *224* (1), 243−252.
(12) Dartois, E.; Engrand, C.; Duprat, J.; Godard, M.; Charon, E.; Delauche, L.; Sandt, C.; Borondics, F. Dome C Ultracarbonaceous Antarctic Micrometeorites - Infrared and Raman Fingerprints. *Astron. Astrophys.* **2018**, *609*, A65.
(13) Bardyn, A.; Baklouti, D.; Cottin, H.; Fray, N.; Briois, C.; Paquette, J.; Stenzel, O.; Engrand, C.; Fischer, H.; Hornung, K.; Isnard, R.; Langevin, Y.; Lehto, H.; Le Roy, L.; Ligier, N.; Merouane, S.; Modica, P.; Orthous-Daunay, F.-R.; Rynö, J.; Schulz, R.; Silén, J.; Thirkell, L.; Varmuza, K.; Zaprudin, B.; Kissel, J.; Hilchenbach, M. Carbon-Rich Dust in Comet 67P/Churyumov-Gerasimenko Measured by COSIMA/Rosetta. *Mon. Not. R. Astron. Soc.* **2017**, *469* (Suppl_2), S712−S722.
(14) Fray, N.; Bardyn, A.; Cottin, H.; Altwegg, K.; Baklouti, D.; Briois, C.; Colangeli, L.; Engrand, C.; Fischer, H.; Glasmachers, A.; Grün, E.; Haerendel, G.; Henkel, H.; Höfner, H.; Hornung, K.; Jessberger, E. K.; Koch, A.; Krüger, H.; Langevin, Y.; Lehto, H.; Lehto, K.; Le Roy, L.; Merouane, S.; Modica, P.; Orthous-Daunay, F.-R.; Paquette, J.; Raulin, F.; Rynö, J.; Schulz, R.; Silén, J.; Siljeström, S.; Steiger, W.; Stenzel, O.; Stephan, T.; Thirkell, L.; Thomas, R.; Torkar, K.; Varmuza, K.; Wanczek, K.-P.; Zaprudin, B.; Kissel, J.; Hilchenbach, M. High-Molecular-Weight Organic Matter in the Particles of Comet 67P/Churyumov−Gerasimenko. *Nature* **2016**, *538* (7623), 72−74.
(15) Harker, D. E.; Wooden, D. H.; Kelley, M. S. P.; Woodward, C. E. Dust Properties of Comets Observed by Spitzer. *Planet Sci. J.* **2023**, *4* (12), 242.
(16) Oba, Y.; Takano, Y.; Furukawa, Y.; Koga, T.; Glavin, D. P.; Dworkin, J. P.; Naraoka, H. Identifying the Wide Diversity of Extraterrestrial Purine and Pyrimidine Nucleobases in Carbonaceous Meteorites. *Nat. Commun.* **2022**, *13* (1), 2008.
(17) Elsila, J. E.; Aponte, J. C.; Blackmond, D. G.; Burton, A. S.; Dworkin, J. P.; Glavin, D. P. Meteoritic Amino Acids: Diversity in Compositions Reflects Parent Body Histories. *ACS Cent. Sci.* **2016**, *2* (6), 370−379.
(18) Elsila, J. E.; Glavin, D. P.; Dworkin, J. P. Cometary Glycine Detected in Samples Returned by Stardust. *Meteorit. Planet. Sci.* **2009**, *44* (9), 1323−1330.
(19) Oba, Y.; Koga, T.; Takano, Y.; Ogawa, N. O.; Ohkouchi, N.; Sasaki, K.; Sato, H.; Glavin, D. P.; Dworkin, J. P.; Naraoka, H.; Tachibana, S.; Yurimoto, H.; Nakamura, T.; Noguchi, T.; Okazaki, R.; Yabuta, H.; Sakamoto, K.; Yada, T.; Nishimura, M.; Nakato, A.; Miyazaki, A.; Yogata, K.; Abe, M.; Okada, T.; Usui, T.; Yoshikawa, M.; Saiki, T.; Tanaka, S.; Terui, F.; Nakazawa, S.; Watanabe, S.; Tsuda, Y. Uracil in the Carbonaceous Asteroid (162173) Ryugu. *Nat. Commun.* **2023**, *14* (1), 1292.
(20) Yada, T.; Abe, M.; Okada, T.; Nakato, A.; Yogata, K.; Miyazaki, A.; Hatakeda, K.; Kumagai, K.; Nishimura, M.; Hitomi, Y.; Soejima, H.; Yoshitake, M.; Iwamae, A.; Furuya, S.; Uesugi, M.; Karouji, Y.; Usui, T.; Hayashi, T.; Yamamoto, D.; Fukai, R.; Sugita, S.; Cho, Y.; Yumoto, K.; Yabe, Y.; Bibring, J.-P.; Pilorget, C.; Hamm, V.; Brunetto, R.; Riu, L.; Lourit, L.; Loizeau, D.; Lequertier, G.; Moussi-Soffys, A.; Tachibana, S.; Sawada, H.; Okazaki, R.; Takano, Y.; Sakamoto, K.; Miura, Y. N.; Yano, H.; Ireland, T. R.; Yamada, T.; Fujimoto, M.; Kitazato, K.; Namiki, N.; Arakawa, M.; Hirata, N.; Yurimoto, H.; Nakamura, T.; Noguchi, T.; Yabuta, H.; Naraoka, H.; Ito, M.; Nakamura, E.; Uesugi, K.; Kobayashi, K.; Michikami, T.; Kikuchi, H.; Hirata, N.; Ishihara, Y.; Matsumoto, K.; Noda, H.; Noguchi, R.; Shimaki, Y.; Shirai, K.; Ogawa, K.; Wada, K.; Senshu, H.; Yamamoto, Y.; Morota, T.; Honda, R.; Honda, C.; Yokota, Y.; Matsuoka, M.; Sakatani, N.; Tatsumi, E.; Miura, A.; Yamada, M.; Fujii, A.; Hirose, C.; Hosoda, S.; Ikeda, H.; Iwata, T.; Kikuchi, S.; Mimasu, Y.; Mori, O.; Ogawa, N.; Ono, G.; Shimada, T.; Soldini, S.; Takahashi, T.; Takei, Y.; Takeuchi, H.; Tsukizaki, R.; Yoshikawa, K.; Terui, F.; Nakazawa, S.; Tanaka, S.; Saiki, T.; Yoshikawa, M.; Watanabe, S.; Tsuda, Y. Preliminary Analysis of the Hayabusa2 Samples Returned from C-Type Asteroid Ryugu. *Nat. Astron.* **2021**, *6* (2), 214−220.
(21) Yabuta, H.; Cody, G. D.; Engrand, C.; Kebukawa, Y.; De Gregorio, B.; Bonal, L.; Remusat, L.; Stroud, R.; Quirico, E.; Nittler, L.; Hashiguchi, M.; Komatsu, M.; Okumura, T.; Mathurin, J.; Dartois, E.; Duprat, J.; Takahashi, Y.; Takeichi, Y.; Kilcoyne, D.; Yamashita, S.; Dazzi, A.; Deniset-Besseau, A.; Sandford, S.; Martins, Z.; Tamenori, Y.; Ohigashi, T.; Suga, H.; Wakabayashi, D.; Verdier-Paoletti, M.; Mostefaoui, S.; Montagnac, G.; Barosch, J.; Kamide, K.; Shigenaka, M.; Bejach, L.; Matsumoto, M.; Enokido, Y.; Noguchi, T.; Yurimoto, H.; Nakamura, T.; Okazaki, R.; Naraoka, H.; Sakamoto, K.; Connolly, H. C.; Lauretta, D. S.; Abe, M.; Okada, T.; Yada, T.; Nishimura, M.; Yogata, K.; Nakato, A.; Yoshitake, M.; Iwamae, A.; Furuya, S.; Hatakeda, K.; Miyazaki, A.; Soejima, H.; Hitomi, Y.; Kumagai, K.; Usui, T.; Hayashi, T.; Yamamoto, D.; Fukai, R.; Sugita, S.; Kitazato, K.; Hirata, N.; Honda, R.; Morota, T.; Tatsumi, E.; Sakatani, N.; Namiki, N.; Matsumoto, K.; Noguchi, R.; Wada, K.; Senshu, H.; Ogawa, K.; Yokota, Y.; Ishihara, Y.; Shimaki, Y.; Yamada, M.; Honda, C.; Michikami, T.; Matsuoka, M.; Hirata, N.; Arakawa, M.; Okamoto, C.; Ishiguro, M.; Jaumann, R.; Bibring, J.-P.; Grott, M.; Schröder, S.; Otto, K.; Pilorget, C.; Schmitz, N.; Biele, J.; Ho, T.-M.; Moussi-Soffys, A.; Miura, A.; Noda, H.; Yamada, T.; Yoshihara, K.; Kawahara, K.; Ikeda, H.; Yamamoto, Y.; Shirai, K.; Kikuchi, S.; Ogawa, N.; Takeuchi, H.; Ono, G.; Mimasu, Y.; Yoshikawa, K.; Takei, Y.; Fujii, A.; Iijima, Y.; Nakazawa, S.; Hosoda, S.; Iwata, T.; Hayakawa, M.; Sawada, H.; Yano, H.; Tsukizaki, R.; Ozaki, M.; Terui, F.; Tanaka, S.; Fujimoto, M.; Yoshikawa, M.; Saiki, T.; Tachibana, S.; Watanabe, S.; Tsuda, Y. Macromolecular Organic Matter in Samples of the Asteroid (162173) Ryugu. *Science* **2023**, *379* (6634), No. eabn9057.
(22) Naraoka, H.; Takano, Y.; Dworkin, J. P.; Oba, Y.; Hamase, K.; Furusho, A.; Ogawa, N. O.; Hashiguchi, M.; Fukushima, K.; Aoki, D.;

https://doi.org/10.1021/acsearthspacechem.3c00311
ACS Earth Space Chem. XXXX, XXX, XXX−XXX

Schmitt-Kopplin, P.; Aponte, J. C.; Parker, E. T.; Glavin, D. P.; McLain, H. L.; Elsila, J. E.; Graham, H. V.; Eiler, J. M.; Orthous-Daunay, F.-R.; Wolters, C.; Isa, J.; Vuitton, V.; Thissen, R.; Sakai, S.; Yoshimura, T.; Koga, T.; Ohkouchi, N.; Chikaraishi, Y.; Sugahara, H.; Mita, H.; Furukawa, Y.; Hertkorn, N.; Ruf, A.; Yurimoto, H.; Nakamura, T.; Noguchi, T.; Okazaki, R.; Yabuta, H.; Sakamoto, K.; Tachibana, S.; Connolly, H. C.; Lauretta, D. S.; Abe, M.; Yada, T.; Nishimura, M.; Yogata, K.; Nakato, A.; Yoshitake, M.; Suzuki, A.; Miyazaki, A.; Furuya, S.; Hatakeda, K.; Soejima, H.; Hitomi, Y.; Kumagai, K.; Usui, T.; Hayashi, T.; Yamamoto, D.; Fukai, R.; Kitazato, K.; Sugita, S.; Namiki, N.; Arakawa, M.; Ikeda, H.; Ishiguro, M.; Hirata, N.; Wada, K.; Ishihara, Y.; Noguchi, R.; Morota, T.; Sakatani, N.; Matsumoto, K.; Senshu, H.; Honda, R.; Tatsumi, E.; Yokota, Y.; Honda, C.; Michikami, T.; Matsuoka, M.; Miura, A.; Noda, H.; Yamada, T.; Yoshihara, K.; Kawahara, K.; Ozaki, M.; Iijima, Y.; Yano, H.; Hayakawa, M.; Iwata, T.; Tsukizaki, R.; Sawada, H.; Hosoda, S.; Ogawa, K.; Okamoto, C.; Hirata, N.; Shirai, K.; Shimaki, Y.; Yamada, M.; Okada, T.; Yamamoto, Y.; Takeuchi, H.; Fujii, A.; Takei, Y.; Yoshikawa, K.; Mimasu, Y.; Ono, G.; Ogawa, N.; Kikuchi, S.; Nakazawa, S.; Terui, F.; Tanaka, S.; Saiki, T.; Yoshikawa, M.; Watanabe, S.; Tsuda, Y. Soluble Organic Molecules in Samples of the Carbonaceous Asteroid (162173) Ryugu. *Science* **2023**, *379* (6634), 789.

(23) Bekaert, D. V.; Derenne, S.; Tissandier, L.; Marrocchi, Y.; Charnoz, S.; Anquetil, C.; Marty, B. High-Temperature Ionization-Induced Synthesis of Biologically Relevant Molecules in the Protosolar Nebula. *Astrophys. J.* **2018**, *859* (2), 142.

(24) Laurent, B.; Roskosz, M.; Remusat, L.; Robert, F.; Leroux, H.; Vezin, H.; Depecker, C.; Nuns, N.; Lefebvre, J.-M. The Deuterium/Hydrogen Distribution in Chondritic Organic Matter Attests to Early Ionizing Irradiation. *Nat. Commun.* **2015**, *6* (1), 8567.

(25) Danger, G.; Vinogradoff, V.; Matzka, M.; Viennet, J.-C.; Remusat, L.; Bernard, S.; Ruf, A.; Le Sergeant d'Hendecourt, L.; Schmitt-Kopplin, P. Exploring the Link between Molecular Cloud Ices and Chondritic Organic Matter in Laboratory. *Nat. Commun.* **2021**, *12* (1), 3538.

(26) Bernstein, M. P.; Moore, M. H.; Elsila, J. E.; Sandford, S. A.; Allamandola, L. J.; Zare, R. N. Side Group Addition to the Polycyclic Aromatic Hydrocarbon Coronene by Proton Irradiation in Cosmic Ice Analogs. *Astrophys. J.* **2003**, *582* (1), L25−L29.

(27) Ciesla, F. J.; Sandford, S. A. Organic Synthesis via Irradiation and Warming of Ice Grains in the Solar Nebula. *Science* **2012**, *336* (6080), 452−454.

(28) Lisse, C. M.; Young, L. A.; Cruikshank, D. P.; Sandford, S. A.; Schmitt, B.; Stern, S. A.; Weaver, H. A.; Umurhan, O.; Pendleton, Y. J.; Keane, J. T.; Gladstone, G. R.; Parker, J. M.; Binzel, R. P.; Earle, A. M.; Horanyi, M.; El-Maarry, M. R.; Cheng, A. F.; Moore, J. M.; McKinnon, W. B.; Grundy, W. M.; Kavelaars, J. J.; Linscott, I. R.; Lyra, W.; Lewis, B. L.; Britt, D. T.; Spencer, J. R.; Olkin, C. B.; McNutt, R. L.; Elliott, H. A.; Dello-Russo, N.; Steckloff, J. K.; Neveu, M.; Mousis, O. On the Origin & Thermal Stability of Arrokoth's and Pluto's Ices. *Icarus* **2021**, *356*, 114072.

(29) Piani, L.; Marrocchi, Y.; Vacher, L. G.; Yurimoto, H.; Bizzarro, M. Origin of Hydrogen Isotopic Variations in Chondritic Water and Organics. *Earth Planet. Sci. Lett.* **2021**, *567*, 117008.

(30) Bergner, J. B.; Öberg, K. I.; Bergin, E. A.; Andrews, S. M.; Blake, G. A.; Carpenter, J. M.; Cleeves, L. I.; Guzmán, V. V.; Huang, J.; Jørgensen, J. K.; Qi, C.; Schwarz, K. R.; Williams, J. P.; Wilner, D. J. An Evolutionary Study of Volatile Chemistry in Protoplanetary Disks. *Astrophys. J.* **2020**, *898* (2), 97.

(31) Dutrey, A.; Di Folco, E.; Guilloteau, S.; Boehler, Y.; Bary, J.; Beck, T.; Beust, H.; Chapillon, E.; Gueth, F.; Huré, J. M.; Pierens, A.; Piétu, V.; Simon, M.; Tang, Y.-W. Possible Planet Formation in the Young, Low-Mass, Multiple Stellar System GG Tau A. *Nature* **2014**, *514* (7524), 600−602.

(32) Messenger, S.; Stadermann, F. J.; Floss, C.; Nittler, L. R.; Mukhopadhyay, S. Isotopic Signatures of Presolar Materials in Interplanetary Dust. *Space Sci. Rev.* **2003**, *106* (1/4), 155−172.

(33) Aléon, J.; Robert, F.; Chaussidon, M.; Marty, B. Nitrogen Isotopic Composition of Macromolecular Organic Matter in Interplanetary Dust Particles. *Geochim. Cosmochim. Acta* **2003**, *67* (19), 3773−3783.

(34) Grossman, L. Condensation in the Primitive Solar Nebula. *Geochim. Cosmochim. Acta* **1972**, *36* (5), 597−619.

(35) Zubko, V.; Dwek, E.; Arendt, R. G. Interstellar Dust Models Consistent with Extinction, Emission, and Abundance Constraints. *Astrophys. J. Suppl. Ser.* **2004**, *152* (2), 211−249.

(36) Pacetti, E.; Turrini, D.; Schisano, E.; Molinari, S.; Fonte, S.; Politi, R.; Hennebelle, P.; Klessen, R.; Testi, L.; Lebreuilly, U. Chemical Diversity in Protoplanetary Disks and Its Impact on the Formation History of Giant Planets. *Astrophys. J.* **2022**, *937* (1), 36.

(37) Henning, T.; Semenov, D. Chemistry in Protoplanetary Disks. *Chem. Rev.* **2013**, *113*, 9016−9042.

(38) Llorca, J.; Casanova, I. Reaction between H2, CO, and H2S over Fe, Ni Metal in the Solar Nebula: Experimental Evidence for the Formation of Sulfur-Bearing Organic Molecules and Sulfides. *Meteorit. Planet. Sci.* **2000**, *35* (4), 841−848.

(39) Nuth, J. A., III; Johnson, N. M.; Manning, S. A Self-Perpetuating Catalyst for the Production of Complex Organic Molecules in Protostellar Nebulae. *Astrophys. J.* **2008**, *673* (2), L225−L228.

(40) Cabedo, V.; Llorca, J.; Trigo-Rodriguez, J. M.; Rimola, A. Study of Fischer−Tropsch-Type Reactions on Chondritic Meteorites. *Astron. Astrophys.* **2021**, *650*, A160.

(41) Cody, G. D.; Heying, E.; Alexander, C. M. O.; Nittler, L. R.; Kilcoyne, A. L. D.; Sandford, S. A.; Stroud, R. M. Establishing a Molecular Relationship between Chondritic and Cometary Organic Solids. *Proc. Natl. Acad. Sci. U.S.A.* **2011**, *108* (48), 19171−19176.

(42) Kebukawa, Y.; David Kilcoyne, A. L.; Cody, G. D. Exploring The Potential Formation Of Organic Solids In Chondrites And Comets Through Polymerization Of Interstellar Formaldehyde. *Astrophys. J.* **2013**, *771* (1), 19.

(43) Hirakawa, N.; Kebukawa, Y.; Furukawa, Y.; Kondo, M.; Nakano, H.; Kobayashi, K. Aqueous Alteration without Initial Water: Possibility of Organic-Induced Hydration of Anhydrous Silicates in Meteorite Parent Bodies. *Earth Planets Space* **2021**, *73* (1), 16.

(44) Vinogradoff, V.; Le Guillou, C.; Bernard, S.; Binet, L.; Cartigny, P.; Brearley, A. J.; Remusat, L. Paris vs. Murchison: Impact of Hydrothermal Alteration on Organic Matter in CM Chondrites. *Geochim. Cosmochim. Acta* **2017**, *212*, 234−252.

(45) Vinogradoff, V.; Bernard, S.; Le Guillou, C.; Remusat, L. Evolution of Interstellar Organic Compounds under Asteroidal Hydrothermal Conditions. *Icarus* **2018**, *305*, 358−370.

(46) Oba, Y.; Takano, Y.; Naraoka, H.; Furukawa, Y.; Glavin, D. P.; Dworkin, J. P.; Tachibana, S. Extraterrestrial Hexamethylenetetramine in Meteorites—a Precursor of Prebiotic Chemistry in the Inner Solar System. *Nat. Commun.* **2020**, *11* (1), 6243.

(47) Marrocchi, Y.; Rigaudier, T.; Piralla, M.; Piani, L. Hydrogen Isotopic Evidence for Nebular Pre-Hydration and the Limited Role of Parent-Body Processes in CM Chondrites. *Earth Planet. Sci. Lett.* **2023**, *611*, 118151.

(48) Kuga, M.; Carrasco, N.; Marty, B.; Marrocchi, Y.; Bernard, S.; Rigaudier, T.; Fleury, B.; Tissandier, L. Nitrogen Isotopic Fractionation during Abiotic Synthesis of Organic Solid Particles. *Earth Planet. Sci. Lett.* **2014**, *393*, 2−13.

(49) Kuga, M.; Cernogora, G.; Marrocchi, Y.; Tissandier, L.; Marty, B. Processes of Noble Gas Elemental and Isotopic Fractionations in Plasma-Produced Organic Solids: Cosmochemical Implications. *Geochim. Cosmochim. Acta* **2017**, *217*, 219−230.

(50) Kuga, M.; Marty, B.; Marrocchi, Y.; Tissandier, L. Synthesis of Refractory Organic Matter in the Ionized Gas Phase of the Solar Nebula. *Proc. Natl. Acad. Sci. U.S.A.* **2015**, *112* (23), 7129−7134.

(51) Lodders, K. *Solar Elemental Abundances*; Oxford Research Encyclopedia of Planetary Science, 2020.

(52) Hörst, S. M. Titan's Atmosphere and Climate. *J. Geophys. Res. Planets* **2017**, *122* (3), 432−482.

https://doi.org/10.1021/acsearthspacechem.3c00311
ACS Earth Space Chem. XXXX, XXX, XXX−XXX

(53) Peeters, Z.; Botta, O.; Charnley, S. B.; Ruiterkamp, R.; Ehrenfreund, P. The Astrobiology of Nucleobases. *Astrophys. J.* **2003**, *593* (2), L129−L132.
(54) Maillard, J.; Carrasco, N.; Schmitz-Afonso, I.; Gautier, T.; Afonso, C. Comparison of Soluble and Insoluble Organic Matter in Analogues of Titan's Aerosols. *Earth Planet. Sci. Lett.* **2018**, *495*, 185−191.
(55) Carrasco, N.; Schmitz-Afonso, I.; Bonnet, J.-Y.; Quirico, E.; Thissen, R.; Dutuit, O.; Bagag, A.; Laprévote, O.; Buch, A.; Giulani, A.; Adandé, G.; Ouni, F.; Hadamcik, E.; Szopa, C.; Cernogora, G. Chemical Characterization of Titan's Tholins: Solubility, Morphology and Molecular Structure Revisited. *J. Phys. Chem. A* **2009**, *113* (42), 11195−11203.
(56) Szopa, C.; Cernogora, G.; Boufendi, L.; Correia, J. J.; Coll, P. PAMPRE: A Dusty Plasma Experiment for Titan's Tholins Production and Study. *Planet. Space Sci.* **2006**, *54* (4), 394−404.
(57) Gautier, T.; Carrasco, N.; Mahjoub, A.; Vinatier, S.; Giuliani, A.; Szopa, C.; Anderson, C. M.; Correia, J.-J.; Dumas, P.; Cernogora, G. Mid- and Far-Infrared Absorption Spectroscopy of Titan's Aerosols Analogues. *Icarus* **2012**, *221* (1), 320−327.
(58) Gautier, T.; Carrasco, N.; Schmitz-Afonso, I.; Touboul, D.; Szopa, C.; Buch, A.; Pernot, P. Nitrogen Incorporation in Titan's Tholins Inferred by High Resolution Orbitrap Mass Spectrometry and Gas Chromatography−Mass Spectrometry. *Earth Planet. Sci. Lett.* **2014**, *404*, 33−42.
(59) Fleury, B.; Carrasco, N.; Gautier, T.; Mahjoub, A.; He, J.; Szopa, C.; Hadamcik, E.; Buch, A.; Cernogora, G. Influence of CO on Titan Atmospheric Reactivity. *Icarus* **2014**, *238*, 221−229.
(60) Carrasco, N.; Jomard, F.; Vigneron, J.; Etcheberry, A.; Cernogora, G. Laboratory Analogues Simulating Titan's Atmospheric Aerosols: Compared Chemical Compositions of Grains and Thin Films. *Planet. Space Sci.* **2016**, *128*, 52−57.
(61) Rüger, C. P.; Maillard, J.; Le Maître, J.; Ridgeway, M.; Thompson, C. J.; Schmitz-Afonso, I.; Gautier, T.; Carrasco, N.; Park, M. A.; Giusti, P.; Afonso, C. Structural Study of Analogues of Titan's Haze by Trapped Ion Mobility Coupled with a Fourier Transform Ion Cyclotron Mass Spectrometer. *J. Am. Soc. Mass Spectrom.* **2019**, *30* (7), 1169−1173.
(62) Jovanović, L.; Gautier, T.; Vuitton, V.; Wolters, C.; Bourgalais, J.; Buch, A.; Orthous-Daunay, F.-R.; Vettier, L.; Flandinet, L.; Carrasco, N. Chemical Composition of Pluto Aerosol Analogues. *Icarus* **2020**, *346*, 113774.
(63) Maillard, J.; Schmitz-Afonso, I.; Gautier, T.; Afonso, C.; Carrasco, N. Suggested Plausible Structures for Titan's Haze Analogs Using Tandem Mass Spectrometry. *Icarus* **2021**, *358*, 114181.
(64) Sueur, M.; Maillard, J.; Lacroix-Andrivet, O.; Rüger, C. P.; Giusti, P.; Lavanant, H.; Afonso, C. PyC2MC: An Open-Source Software Solution for Visualization and Treatment of High-Resolution Mass Spectrometry Data. *J. Am. Soc. Mass Spectrom.* **2023**, *34*, 617−626.
(65) Joshi, Y. V.; Mennito, A. S.; Brown, S. H.; Qian, K. Ultra-Low Hydrogen Content Bowl-Shaped Polycyclic Aromatic Hydrocarbons in Petroleum. *Fuel* **2021**, *301*, 121066.
(66) Danger, G.; Ruf, A.; Maillard, J.; Hertzog, J.; Vinogradoff, V.; Schmitt-Kopplin, P.; Afonso, C.; Carrasco, N.; Schmitz-Afonso, I.; d'Hendecourt, L. L. S.; Remusat, L. Unprecedented Molecular Diversity Revealed in Meteoritic Insoluble Organic Matter: The Paris Meteorite's Case. *Planet. Sci. J.* **2020**, *1* (3), 55.
(67) Yassine, M. M.; Harir, M.; Dabek-Zlotorzynska, E.; Schmitt-Kopplin, P. Structural Characterization of Organic Aerosol Using Fourier Transform Ion Cyclotron Resonance Mass Spectrometry: Aromaticity Equivalent Approach. *Rapid Commun. Mass Spectrom.* **2014**, *28* (22), 2445−2454.
(68) Kuga, M. Origine des fractionnements isotopiques de l'azote et des gaz rares dans les météorites et les atmosphères planétaires. Ph.D. Dissertation, Université de Lorraine, Nancy, 2014.
(69) Yung, Y. L.; Allen, M.; Pinto, J. P. Photochemistry of the Atmosphere of Titan - Comparison between Model and Observations. *Astrophys. J. Suppl. Ser.* **1984**, *55*, 465−506.
(70) Barnes, J. W.; Turtle, E. P.; Trainer, M. G.; Lorenz, R. D.; MacKenzie, S. M.; Brinckerhoff, W. B.; Cable, M. L.; Ernst, C. M.; Freissinet, C.; Hand, K. P.; Hayes, A. G.; Hörst, S. M.; Johnson, J. R.; Karkoschka, E.; Lawrence, D. J.; Le Gall, A.; Lora, J. M.; McKay, C. P.; Miller, R. S.; Murchie, S. L.; Neish, C. D.; Newman, C. E.; Núñez, J.; Panning, M. P.; Parsons, A. M.; Peplowski, P. N.; Quick, L. C.; Radebaugh, J.; Rafkin, S. C. R.; Shiraishi, H.; Soderblom, J. M.; Sotzen, K. S.; Stickle, A. M.; Stofan, E. R.; Szopa, C.; Tokano, T.; Wagner, T.; Wilson, C.; Yingst, R. A.; Zacny, K.; Stähler, S. C. Science Goals and Objectives for the Dragonfly Titan Rotorcraft Relocatable Lander. *Planet. Sci. J.* **2021**, *2* (4), 130.
(71) Maillard, J.; Hupin, S.; Carrasco, N.; Schmitz-Afonso, I.; Gautier, T.; Afonso, C. Structural Elucidation of Soluble Organic Matter: Application to Titan's Haze. *Icarus* **2020**, *340*, 113627.
(72) Néri, A.; Guyot, F.; Reynard, B.; Sotin, C. A Carbonaceous Chondrite and Cometary Origin for Icy Moons of Jupiter and Saturn. *Earth Planet. Sci. Lett.* **2020**, *530*, 115920.
(73) Reynard, B.; Sotin, C. Carbon-Rich Icy Moons and Dwarf Planets. *Earth Planet. Sci. Lett.* **2023**, *612*, 118172.

https://doi.org/10.1021/acsearthspacechem.3c00311
ACS Earth Space Chem. XXXX, XXX, XXX−XXX